

Activation of Sympathetic Signaling in Macrophages Blocks Systemic Inflammation and Protects against Renal Ischemia-Reperfusion Injury

Sho Hasegawa ^{1,2} Tsuyoshi Inoue^{2,3}, Yasuna Nakamura,^{1,3} Daichi Fukaya,^{2,4} Rie Uni,^{1,2} Chia-Hsien Wu ^{1,3} Rie Fujii,^{1,2} Wachirasek Peerapanyasut,^{2,5} Akashi Taguchi,⁶ Takahide Kohro,⁷ Shintaro Yamada,^{8,9} Mikako Katagiri,⁸ Toshiyuki Ko,^{8,9} Seitaro Nomura,^{8,9} Atsuko Nakanishi Ozeki,⁶ Etsuo A. Susaki,^{10,11} Hiroki R. Ueda,^{10,11} Nobuyoshi Akimitsu,⁶ Youichiro Wada,⁶ Issei Komuro,⁸ Masaomi Nangaku,¹ and Reiko Inagi,²

Due to the number of contributing authors, the affiliations are listed at the end of this article.

ABSTRACT

Background The sympathetic nervous system regulates immune cell dynamics. However, the detailed role of sympathetic signaling in inflammatory diseases is still unclear because it varies according to the disease situation and responsible cell types. This study focused on identifying the functions of sympathetic signaling in macrophages in LPS-induced sepsis and renal ischemia-reperfusion injury (IRI).

Methods We performed RNA sequencing of mouse macrophage cell lines to identify the critical gene that mediates the anti-inflammatory effect of β 2-adrenergic receptor (*Adrb2*) signaling. We also examined the effects of salbutamol (a selective *Adrb2* agonist) in LPS-induced systemic inflammation and renal IRI. Macrophage-specific *Adrb2* conditional knockout (cKO) mice and the adoptive transfer of salbutamol-treated macrophages were used to assess the involvement of macrophage *Adrb2* signaling.

Results *In vitro*, activation of *Adrb2* signaling in macrophages induced the expression of T cell Ig and mucin domain 3 (*Tim3*), which contributes to anti-inflammatory phenotypic alterations. *In vivo*, salbutamol administration blocked LPS-induced systemic inflammation and protected against renal IRI; this protection was mitigated in macrophage-specific *Adrb2* cKO mice. The adoptive transfer of salbutamol-treated macrophages also protected against renal IRI. Single-cell RNA sequencing revealed that this protection was associated with the accumulation of *Tim3*-expressing macrophages in the renal tissue.

Conclusions The activation of *Adrb2* signaling in macrophages induces anti-inflammatory phenotypic alterations partially via the induction of *Tim3* expression, which blocks LPS-induced systemic inflammation and protects against renal IRI.

JASN 32: 1599–1615, 2021. doi: <https://doi.org/10.1681/ASN.2020121723>

The sympathetic nervous system (SNS) plays important roles in the maintenance of homeostasis. The SNS is known to innervate lymphoid organs, including the spleen and lymph nodes.^{1,2} This anatomic finding suggests that sympathetic neurotransmitters directly affect immune cell dynamics. Although many previous reports have clarified that SNS activity certainly affects immune systems,^{3,4} the direction of its immunologic regulation is not straightforward and varies according to the disease situation and responsible cell types. For example,

Received December 09, 2020; Accepted February 15, 2021.

Published online ahead of print. Publication date available at www.jasn.org.

Correspondence: Dr. Tsuyoshi Inoue, Department of Physiology of Visceral Function and Body Fluid, Nagasaki University Graduate School of Biomedical Sciences, 3F Basic Medical Science Building, 1-12-4, Sakamoto, Nagasaki 852-8523, Japan. Email: ts-inoue@nagasaki-u.ac.jp

Copyright © 2021 by the American Society of Nephrology

activation of sympathetic signaling enhances retention-promoting signals and consequently inhibits lymphocyte egress from lymph nodes (anti-inflammatory direction).⁵ In contrast, SNS activation induces the accumulation of pathogenic CD4-positive T cells in the fifth lumbar cord, which is involved in the pathogenesis of experimental autoimmune encephalomyelitis (proinflammatory direction).⁶ Moreover, adrenergic receptors, which receive sympathetic signaling, are ubiquitously expressed in various cell types in the body, which makes it difficult to precisely understand the sympathetic regulation of inflammatory diseases. Thus, the effect of sympathetic signal activation *in vivo* is heterogeneous, and “the critical receiver of sympathetic signaling (immune cells, epithelial cells, or other cell types)” may differ depending on the situation.

Therefore, it is important to clarify the detailed role of sympathetic signaling in specific cell types in specific inflammatory situations. Hence, in this study, we focused on sympathetic signaling in macrophages and sought to determine its detailed roles in systemic inflammation (LPS-induced sepsis) and local inflammation (renal ischemia-reperfusion injury).

METHODS

Cell Culture and Reagents

RAW 264.7 cells (mouse macrophage cell line) were maintained in DMEM-high-glucose media (D5796; Sigma-Aldrich, St. Louis, MO) containing 10% FBS (F7524, lot #BCBT 3830; Sigma-Aldrich). U937 cells (human monocyte cell line) were maintained in RPMI-1640 media (R8758; Sigma-Aldrich) with 10% FBS. U937 cells were differentiated into macrophages by 48-hour stimulation with 100 nM phorbol 12-myristate 13-acetate (P1585; Sigma-Aldrich). All cells were cultured in a humidified 5% CO₂-enriched atmosphere at 37°C. TNF- α was induced by 100 ng/ml LPS (L4391; Sigma-Aldrich). L-NE (25304-31; Nacalai tesque, Kyoto, Japan), salbutamol (S8260; Sigma-Aldrich), butoxamine hydrochloride (B1385; Sigma-Aldrich), and the protein kinase A (PKA) inhibitor 14-22 amide (476485; Sigma-Aldrich) were used in this study.

Measurement of TNF- α and ILs

The TNF- α concentration was measured using TNF- α Mouse Uncoated ELISA Kit with Plates (88-7324-22; Thermo Fisher Scientific, Waltham, MA) or TNF- α Human Uncoated ELISA Kit with Plates (88-7346-86; Thermo Fisher Scientific) according to the manufacturer's protocol. The concentrations of IL-6 and IL-10 were measured using Mouse IL-6 ELISA Kit (KE10007; Proteintech, Rosemont, IL) and Mouse IL-10 ELISA Kit (KE10008; Proteintech).

RNA Sequencing

Total RNA was isolated using the RNeasy Mini Kit (74106; Qiagen, Hilden, Germany). Poly (A)-containing mRNA

Significance Statement

The detailed role of neural activity in inflammatory diseases is still unclear because it varies according to the disease situation and responsible cell types. This study shows that activation of β 2-adrenergic receptor (*Adrb2*) signaling in macrophages induces the expression of T cell Ig and mucin domain 3 (*Tim3*), which contributes to anti-inflammatory phenotypic alterations. Experiments using conditional knockout mice reveal that macrophage *Adrb2* signaling directly mitigates LPS-induced systemic inflammation and renal ischemia-reperfusion injury (IRI). The adoptive transfer of *Adrb2* signal-activated macrophages also protects against renal IRI, in association with the accumulation of *Tim3*-expressing macrophages in the renal tissue. These results indicate that macrophage *Adrb2* signaling plays critical roles in the severity of AKI.

molecules were isolated from the total RNA and then converted to cDNA with poly A primers using a TruSeq RNA Sample Preparation kit v2 (Illumina). High-throughput sequencing was performed using a HiSeq2500 (Illumina) system. Sequenced paired-end reads were mapped onto the mouse genome build mm10 using hisat2 with the parameter “-q-dta-cufflinks.” The SAM file was converted into BAM format, and the fragments per kilobase of transcript per million mapped fragments were subsequently calculated using cuffdiff and cummerbund. Genes commonly induced by β 2-adrenergic receptor (*Adrb2*) signaling were extracted using the log fold change, which was calculated from log(fragments per kilobase of transcript per million mapped fragments + 0.001) counts. The data were deposited in the Genomic Expression Archive (GEA) under accession number E-GEAD-404.

Quantitative Real-Time PCR

Total RNA was isolated using the RNeasy Mini Kit (74106) and reverse transcribed using PrimeScript RT master mix (Takara, Shiga, Japan). The cDNA was then subjected to quantitative real-time PCR (qPCR) using the THUNDERBIRD qPCR Mix (Toyobo, Tokyo, Japan) and a CFX96 Real Time System (Bio-Rad). β -actin was used to standardize the mRNA expression levels. The primer sequences are listed in Supplemental Table 1.

Small Interfering RNA Transfection

Small interfering RNA (siRNA) transfection was conducted using Opti-MEM I Reduced Serum Medium (31985070; Thermo Fisher Scientific) and Lipofectamine RNAiMAX Transfection Reagent (13778150; Thermo Fisher Scientific). T cell Ig and mucin domain 3 (*Tim3*) knockdown was conducted by Silencer Select Pre-Designed siRNA for mouse *Tim3* (s101150 [#1] and s101148 [#2]; Thermo Fisher Scientific). Silencer Select Negative Control No. 1 siRNA (4390843; Thermo Fisher Scientific) was used as the negative control.

Gene Overexpression

Tim3 (*Havcr2*) plasmid (green fluorescent protein tagged; MG227499; Origene Technologies, Inc., Rockville, MD) or

empty plasmid was introduced using a Neon Transfection System (Thermo Fisher Scientific) according to the manufacturer's protocol. The overexpression of *Tim3* was validated by immunocytochemistry.

Animal Experiments

Male mice (8–12 weeks of age, 20–25 g) were used for all experiments. Wild-type (WT) C57BL/6 mice were purchased from Nippon Bio-Supp. Center (Tokyo, Japan). Macrophage-specific *Adrb2* conditional knockout (cKO) mice were generated by crossbreeding lysozyme M (*LysM*)-*Cre* and *Adrb2 flox* mice. Genotyping was confirmed by tail PCR using published primers. *LysM-Cre* mice were obtained from the Jackson Laboratory (Bar Harbor, ME). *Adrb2 flox* mice⁷ were provided by Wataru Ogawa (Kobe University, Kobe, Japan) and Gerard Karsenty (Columbia University, New York, NY). All experiments were approved by the University of Tokyo Institutional Review Board (approval nos. P18–051 and H19–164). All animal procedures were performed according to the National Institutes of Health guidelines (Guide for the Care and Use of the Laboratory Animals). BUN and plasma creatinine (Cre) levels were measured by SRL Inc. (Osaka, Japan).

Preparation of Peritoneal Macrophages

After the mouse was euthanized, 8 ml of sterile PBS was injected into the peritoneal cavity. The injected fluid was collected after a gentle massage of the peritoneum. The fluid was centrifuged at 500×g for 5 minutes, and the supernatant was discarded. The cell pellets were resuspended in RPMI-1640 media (R8758; Sigma-Aldrich) with 10% FBS and 1% penicillin-streptomycin, and they were plated in culture dishes. The cells were washed with PBS 1 hour after plating, and the culture medium was refreshed. The next day, the cells were used for experiments.

Renal Bilateral Ischemia-Reperfusion Injury

Mice were anesthetized by the intraperitoneal administration of medetomidine 0.3 mg/kg, butorphanol 5 mg/kg, and midazolam 4 mg/kg. Renal bilateral ischemia-reperfusion injury (bIRI) was performed by clamping the renal pedicles for 26 minutes. The clamps were removed, and the wound was sutured after restoration of blood flow was visually observed. Sham-operated mice underwent the same procedure, without clamping of the renal pedicles.

Splenectomy

Mice were anesthetized by the intraperitoneal administration of medetomidine 0.3 mg/kg, butorphanol 5 mg/kg, and midazolam 4 mg/kg. The splenic vasculature was ligated, and the spleen was removed *via* a small incision.

Immunohistochemistry

Kidney samples were fixed in Mildform 10 N (133–10311; Wako, Osaka, Japan) before being embedded in paraffin. Tissue sections were subjected to periodic acid–Schiff staining for the histologic

examination of tubular necrosis. Semiquantitative tubular injury scores were graded on the basis of the proportion of injured tubules as follows: (0) none, (1) <25%, (2) 25%–50%, (3) 50%–75%, and (4) >75%. The average score of four fields in the outer medulla was calculated for each sample.

For Tim3 immunostaining, anti-Tim3 rabbit mAb (1:200, 83882S; Cell Signaling, Danvers, MA) was used as the primary antibody. The sections were stained with Histofine Simple Stain Mouse MAX PO (R) (414341; Nichirei, Tokyo, Japan) and ImmPACT DAB substrate (SK-4105; Vector, Burlingame, CA), which were then counterstained with Mayer Hematoxylin (Wako).

Three-Dimensional Visualization of the SNS in the Spleen

Three-dimensional (3D) visualization of the SNS in the spleen was performed using Clear, Unobstructed Brain/Body Imaging Cocktails and Computational (CUBIC)^{8–10} analysis as described in our previous papers.^{11,12} In brief, the fixed mouse spleen was immersed in CUBIC-L for delipidation and then subjected to immunofluorescence staining. Finally, the refractive index was matched by the placement of the sample in CUBIC-R+. The primary antibody used for staining was antityrosine hydroxylase antibody (sheep polyclonal, 1:100, ab113; Abcam, Cambridge, United Kingdom). The secondary antibody was Alexa Fluor 555-conjugated donkey anti-sheep IgG (1:100, A-21436; Invitrogen, Carlsbad, CA). The raw image data were acquired with a custom-built light sheet fluorescence microscopy (MVX10-LS; developed by Olympus, Tokyo, Japan). The 3D-rendered image was visualized with Imaris (Bitplane).

Adoptive Transfer of Splenic Macrophages

Spleens were harvested from donor mice, and single-cell suspensions were made through a 40- μ m cell strainer with sterile PBS. The single-cell suspensions were labeled with anti-F4/80 MicroBeads (130–110–443; Miltenyi Biotec, Bergisch Gladbach, Germany), and F4/80-positive splenocytes were selected by the magnetic cell separation method. The cells were incubated with vehicle or 100 μ M salbutamol for 1 hour, and they were washed twice with PBS. The macrophages were intravenously administered to recipient mice.

Single-Cell RNA Sequencing

Digestion buffer was prepared as a mixture of DMEM–high-glucose media (D5796) with 10% FBS (F7524, lot #BCBT 3830), RQ1 RNase-Free DNase (20 U/ml, M6101; Promega, Madison, WI), collagenase type 1 (2 mg/ml, CLS1; Worthington, Columbus, OH), collagenase type 2 (2 mg/ml, CLS2, Worthington), and Dispase II (1 mg/ml, 04942078001; Roche, Mannheim, Germany). Kidneys were harvested, minced into 1-mm³ cubes, and digested using the digestion buffer with shaking at 37°C. The supernatant buffer was collected after shaking for 10 minutes, and fresh digestion buffer was added to the remaining cell aggregations. After this process was

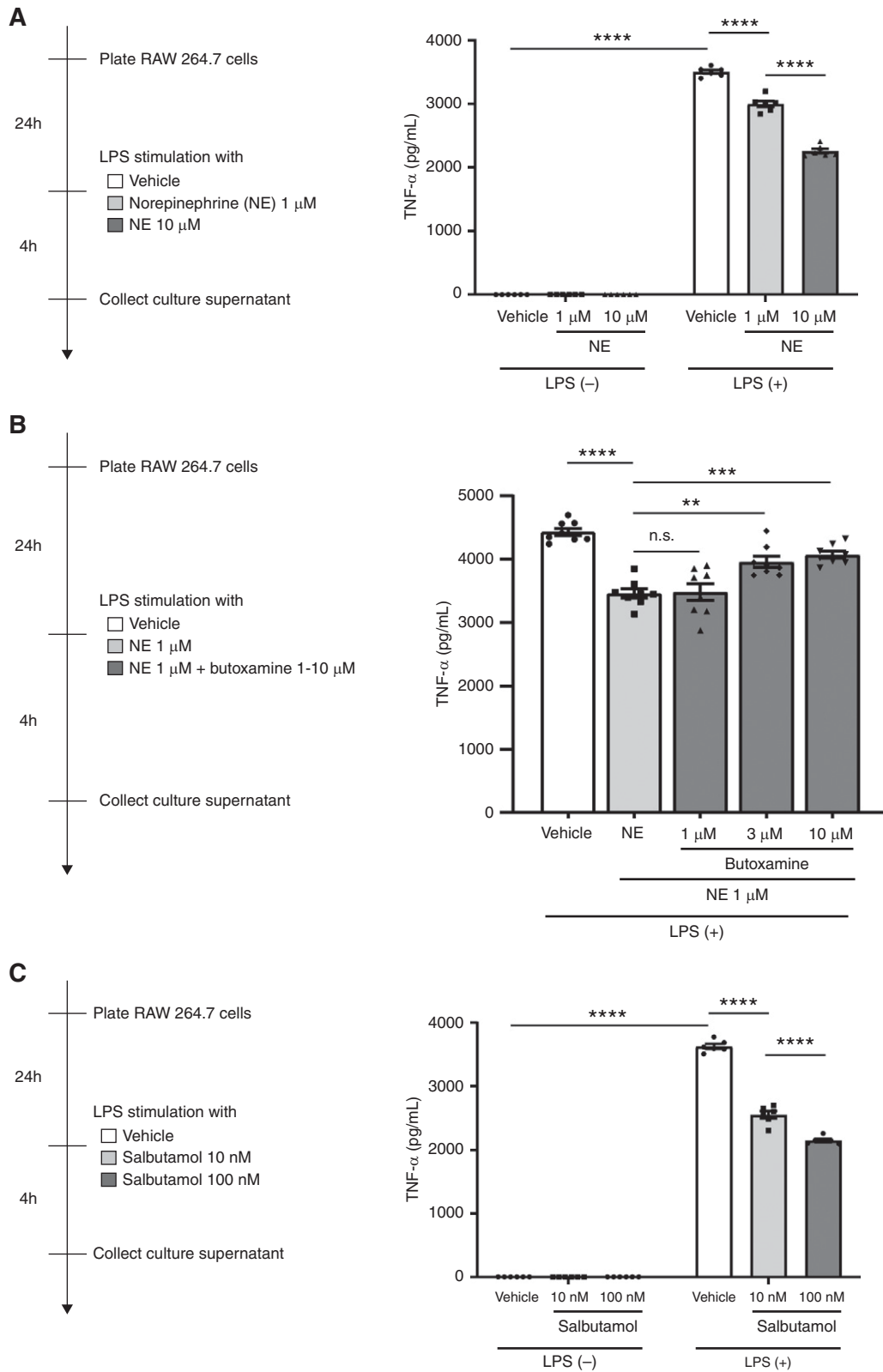


Figure 1. Activation of sympathetic signaling suppresses the inflammatory response of macrophages via Adrb2. (A) TNF- α induction by LPS was suppressed by NE treatment in RAW 264.7 cells ($n=6$). (B) Butoxamine mitigated the anti-inflammatory effect of NE in RAW 264.7 cells ($n=8$). (C) Salbutamol also suppressed TNF- α induction by LPS in RAW 264.7 cells ($n=6$). All data are presented as means \pm SEM. Statistical comparisons were analyzed by (B) one-way ANOVA or (A and C) two-way ANOVA with a post hoc Tukey multiple comparisons test. n.s., not significant. ** $P<0.01$; *** $P<0.001$; **** $P<0.0001$.

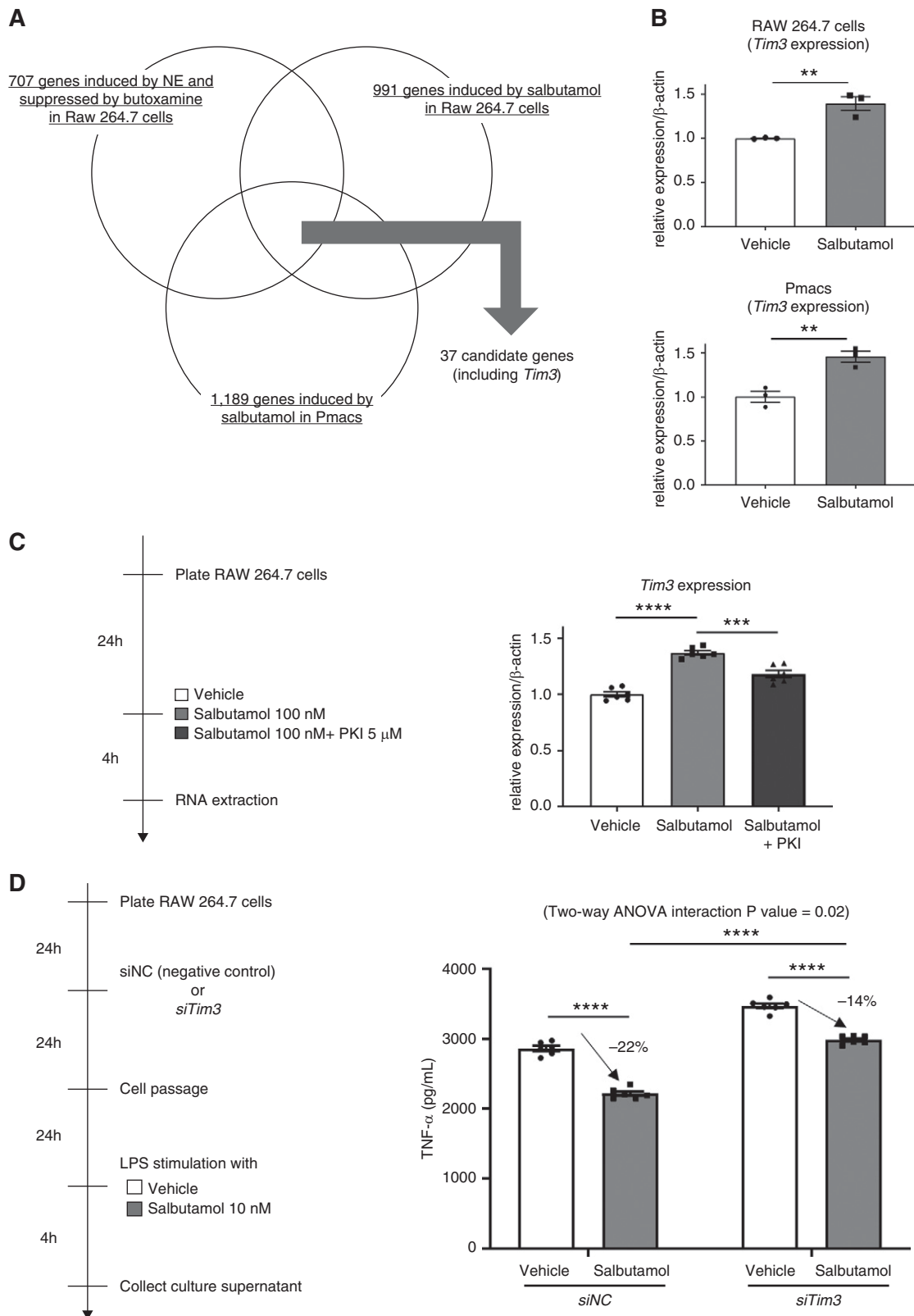


Figure 2. *Tim3* is downstream of *Adrb2* signaling and partially mediates its anti-inflammatory effects. (A) RNA sequencing was conducted for three different *in vitro* macrophage models. The detailed experiment protocols are shown in Supplemental Figure 3: (1) 707 genes were extracted with log fold change (log FC) more than one (NE per vehicle) and log FC less than zero (NE + butoxamine/NE), (2) 991 genes were extracted with log FC more than one (salbutamol per vehicle), and (3) 1189 genes were extracted

repeated four times, the solution was passed through 70- and 40- μm cell strainers successively. The solution was then centrifuged at $300\times g$ for 5 minutes, and the resulting cell pellet was diluted with the digestion buffer again. The solution was passed through 40- μm cell strainers three times, and a single-cell suspension was obtained.

The single-cell suspension was loaded onto a well on the $10\times$ Chromium Single Cell instrument ($10\times$ Genomics, Pleasanton, CA). Bar coding and cDNA synthesis were performed using Chromium Single Cell 3' Reagent Kits v3.1 ($10\times$ Genomics) according to the manufacturer's instructions. High-throughput sequencing was performed using a NovaSeq6000 (Illumina) system at Takara Bio Inc. (Shiga, Japan).

Data Processing and Analysis of Single-Cell RNA-Sequencing Data

The raw data were processed using Cell Ranger v3.1 ($10\times$ Genomics) to obtain the filtered feature bar code matrices. Seurat v3 was used for the detailed analysis. We analyzed each sample separately and excluded cells with <200 or >5000 genes detected or with $<20,000$ unique molecular identifiers detected. We also excluded cells with a relatively high percentage of genes mapped to mitochondrial genes ($\geq 50\%$). Subsequently, we log normalized the data and obtained 2000 highly variable genes for principal component analysis (PCA) from each dataset with "FindVariableFeatures." We then merged the list with the standard workflow using "FindIntegrationAnchors" and "IntegrateData." We subsequently performed PCA for the integrated data using the variable genes and determined significant principal components on the basis of the jackstraw. Clustering was performed using "FindNeighbors" and subsequently, "FindClusters" with a resolution of 0.6. We visualized the data on t-distributed stochastic neighbor embedding (tSNE) using "RunTSNE." Marker genes in each cluster were identified using "FindAllMarkers" with $\text{min.pct}=0.25$ and $\text{logfc.threshold}=0.25$. The marker genes sorted by the average log fold change are presented in Supplemental Table 2. Macrophage subclustering was performed as follows. First, we extracted the macrophage cluster and changed the default assay from "integrated" to "RNA." Then, we log normalized the data and obtained 2000 highly variable genes for PCA with "FindVariableFeatures." Clustering was performed using "FindNeighbors" and subsequently, "FindClusters" with a resolution of 0.8. We visualized the data on tSNE using

"RunTSNE." The data were deposited in the GEA under accession number E-GEAD-405.

Statistical Analyses

All data are presented as means \pm SEM. An unpaired two-tailed *t* test was used to analyze the data for only two groups. For multiplex comparisons, a one-way or two-way ANOVA followed by a *post hoc* Tukey multiple comparisons test, if appropriate, was applied. $P<0.05$ was considered statistically significant. All statistical analyses were performed with GraphPad Prism 8 software (GraphPad Software, San Diego, CA).

RESULTS

Activation of Sympathetic Signaling Suppresses the Inflammatory Response of Macrophages via Adrb2

We first examined the effects of sympathetic signaling on the inflammatory response of macrophages using RAW 264.7 cells (mouse macrophage cell line). Norepinephrine (NE), a sympathetic neurotransmitter, suppressed TNF- α induction by LPS in a dose-dependent manner (Figure 1A). This anti-inflammatory effect was mitigated by butoxamine, a selective Adrb2 antagonist (Figure 1B). The dose-dependent anti-inflammatory effect was also induced by salbutamol, a selective Adrb2 agonist (Figure 1C, Supplemental Figure 1). Thus, activation of sympathetic signaling suppresses the inflammatory response of macrophages via Adrb2. Furthermore, we conducted the same experiment using mouse peritoneal macrophages and differentiated U937 cells (human macrophages) and confirmed that the anti-inflammatory effect of Adrb2 signaling was common in macrophages of various origins (Supplemental Figure 2).

Tim3 Is a Mediator of Anti-Inflammatory Effect Induced by Adrb2 Signaling

We attempted to identify the critical gene that mediates the anti-inflammatory effect of Adrb2 signaling. RNA sequencing was conducted for three different *in vitro* macrophage models. Adrb2 signaling-induced genes were respectively selected in each model: (1) 707 genes, (2) 991 genes, and (3) 1189 genes (Figure 2A, Supplemental Figure 3). Among 37 genes, which were commonly selected in the three models (Supplemental Table 3), we focused on *Tim3*, given its reported anti-inflammatory role in immune cells. qPCR also confirmed

with log FC more than one (salbutamol per vehicle). A total of 37 genes, including *Tim3*, were commonly induced by the activation of Adrb2 signaling in the three different models. (B) qPCR confirmed that *Tim3* expression was upregulated by the salbutamol treatment in RAW 264.7 cells and peritoneal macrophages (Pmacs; $n=3$). (C) *Tim3* induction by salbutamol was counteracted by the inhibition of PKA in RAW 264.7 cells ($n=6$). (D) *Tim3* knockdown by siRNA partly inhibited the anti-inflammatory effect of salbutamol in RAW 264.7 cells ($n=6$). All data are presented as means \pm SEM. (B) An unpaired two-tailed *t* test was used to analyze the data for only two groups. For multiplex comparisons, (C) a one-way ANOVA or two-way (D) ANOVA with a *post hoc* Tukey multiple comparisons test was applied. PKI, protein kinase A inhibitor; siNC, negative control siRNA; siTim3, *Tim3* knockdown by siRNA. ** $P<0.01$; *** $P<0.001$; **** $P<0.0001$.

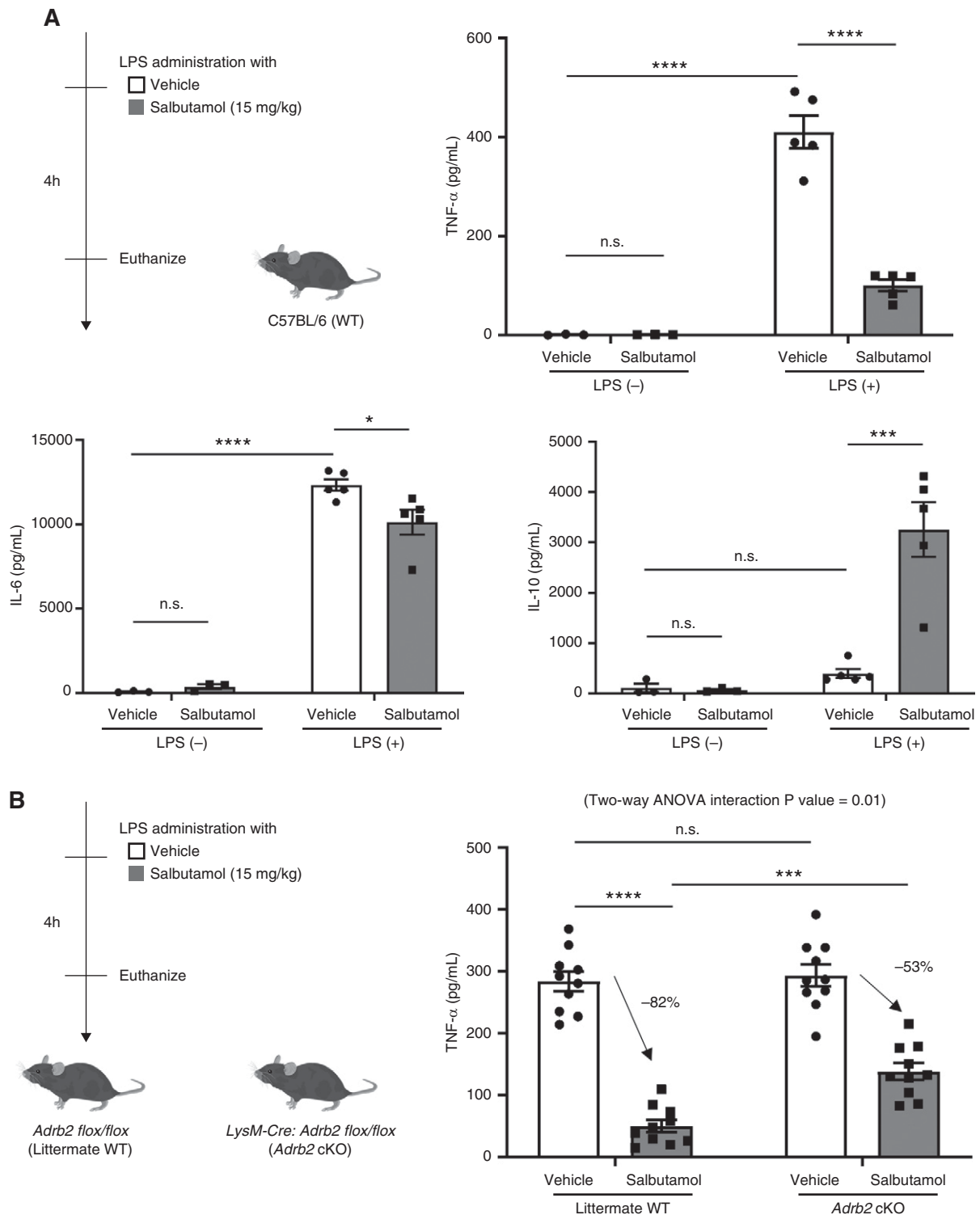


Figure 3. *Adrb2* signaling in macrophages plays a critical role in the *in vivo* systemic inflammatory response. (A) LPS was intraperitoneally administered to WT mice immediately after the intraperitoneal administration of vehicle or salbutamol. Plasma TNF- α and IL-6 levels were reduced, whereas plasma IL-10 level was increased by the salbutamol treatment ($n=3$ or $n=5$). (B) Macrophage-specific *Adrb2* cKO mice were generated by crossbreeding *LysM-Cre* and *Adrb2 flox/flox* mice. LPS was intraperitoneally administered to *Adrb2* cKO mice and their littermate WT mice immediately after the intraperitoneal administration of vehicle or salbutamol. Deletion of *Adrb2* on macrophages partially abolished the salbutamol-induced suppression of the systemic inflammatory response ($n=10$). All data are presented as means \pm SEM. Statistical comparisons were analyzed by a two-way ANOVA with a *post hoc* Tukey multiple comparisons test. n.s., not significant. * $P<0.05$; *** $P<0.001$; **** $P<0.0001$.

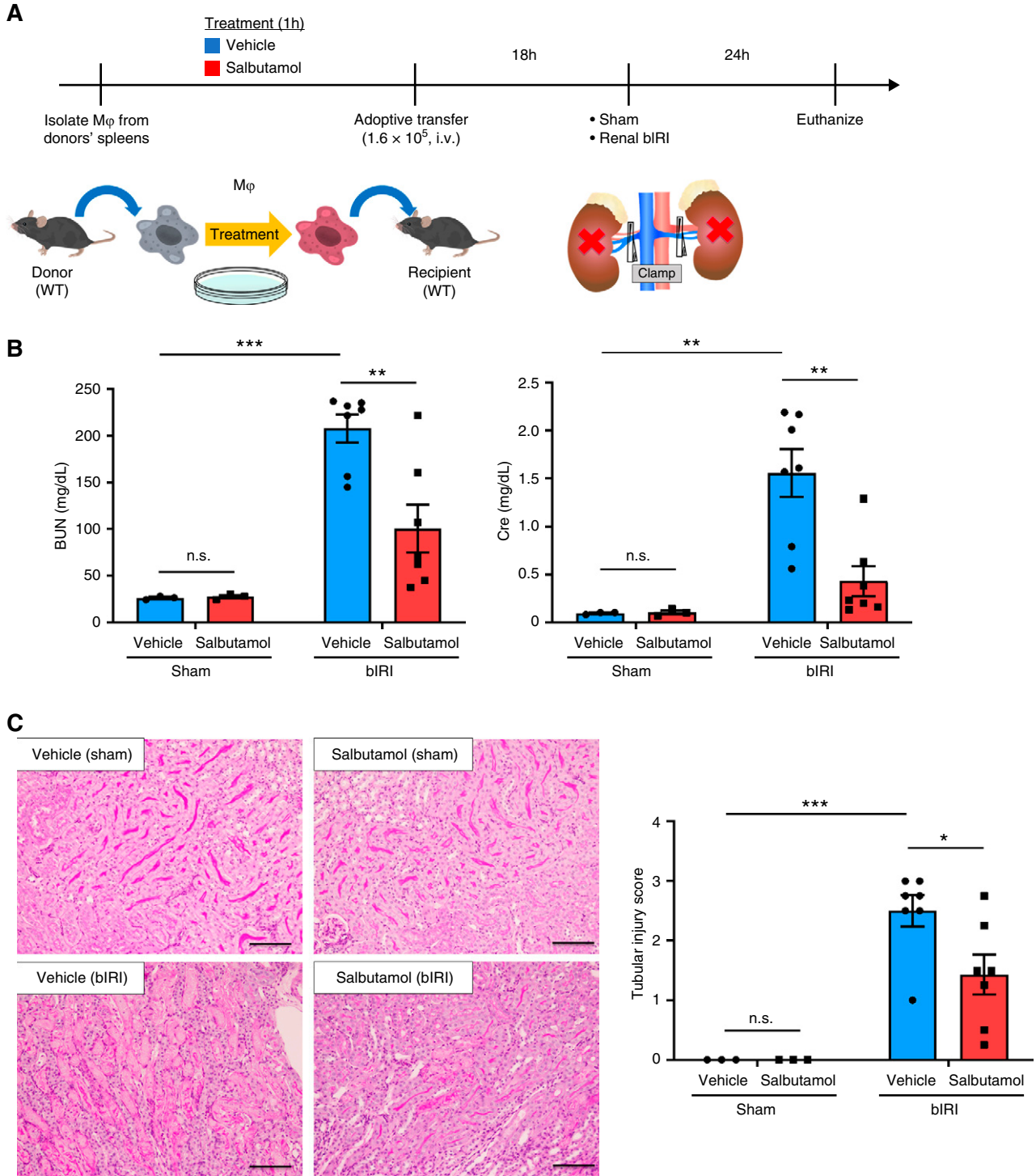


Figure 6. Adoptive transfer of salbutamol-treated macrophages protects against renal ischemia-reperfusion injury. (A) The study protocol is shown. Salbutamol-treated macrophages from donor mice were adoptively transferred to recipient mice 18 hours before bIRI. Blood and kidney samples were obtained 24 hours after bIRI. (B) BUN and plasma Cre levels are shown ($n=3$ or $n=7$). (C) Representative periodic acid–Schiff staining of the renal outer medulla and histologic tubular injury scores are shown ($n=3$ or $n=7$). All data are presented as means \pm SEM. Statistical comparisons were analyzed by a two-way ANOVA with a *post hoc* Tukey multiple comparisons test. M ϕ , macrophage; n.s., not significant; i.v., intravenous. Scale bars: 100 μ m. * $P<0.05$; ** $P<0.01$; *** $P<0.001$.

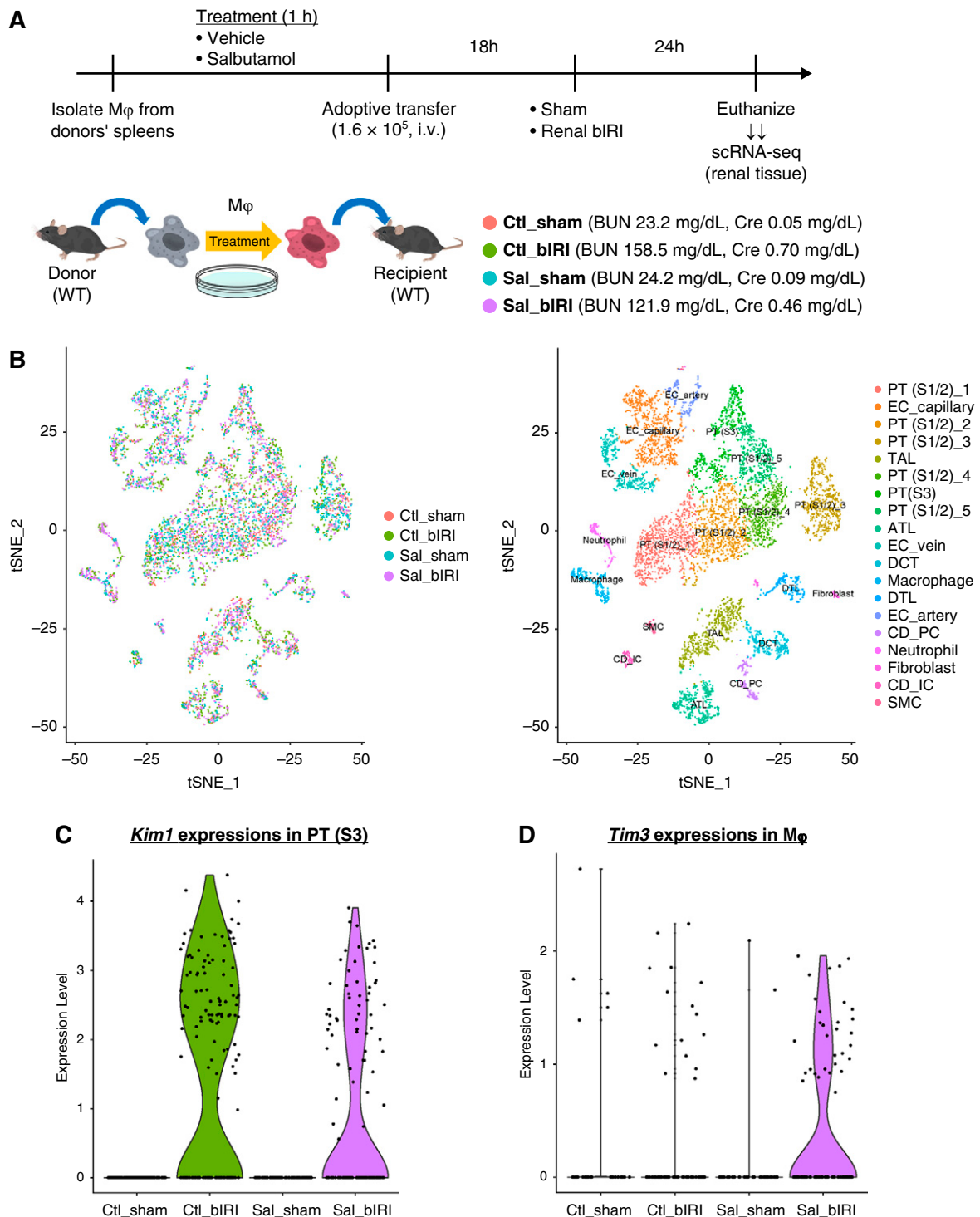


Figure 7. *Tim3*-expressing macrophages are accumulated in the injured kidney after salbutamol-treated macrophage transfer. (A) The study protocol is shown. Four renal tissues from the adoptive transfer experiment were analyzed by scRNA-seq. The BUN and plasma Cre levels of each mouse are shown. (B) tSNE plots of the single-cell data are visualized with sample information (left panel) and cell-type information (right panel). The total numbers of cells in each sample are as follows: 1667 cells (sham operation after vehicle-treated macrophage transfer [Ctl_sham]), 2128 cells (bilateral ischemia-reperfusion injury after vehicle-treated macrophage transfer [Ctl_bIRI]), 1653 cells (sham operation after salbutamol-treated macrophage transfer [Sal_sham]), and 1932 cells (bilateral ischemia-reperfusion injury after salbutamol-treated macrophage transfer [Sal_bIRI]). (C) The violin plot of kidney injury molecule 1 (*Kim1*) expressions in the PT (S3) cluster is drawn. The total numbers of cells in this cluster are as follows: 128 cells (Ctl_sham), 139 cells (Ctl_bIRI), 93 cells (Sal_sham),

LPS administration (Figure 3A). As a result, plasma TNF- α and IL-6 levels were significantly lower in the salbutamol-treated group than in the vehicle-treated group, whereas the level of IL-10, an anti-inflammatory cytokine, was higher in the salbutamol-treated group. Although renal histologic injury was not apparently observed at this stage, the expression of neutrophil gelatinase-associated lipocalin, one of the AKI biomarkers, was significantly reduced in the salbutamol-treated group, suggesting the protective effects of *Adrb2* signaling against kidney injury (Supplemental Figure 7).

However, we were unable to determine whether the systemic anti-inflammatory effect of salbutamol was associated with macrophages because sympathetic signaling plays various physiologic roles in many cell types in the body. Thus, we generated macrophage-specific *Adrb2* cKO mice by crossbreeding *LysM-Cre* and *Adrb2 flox* mice and conducted the same experiment (Figure 3B). Deletion of *Adrb2* on macrophages then partially abolished the salbutamol-induced suppression of the systemic inflammatory response, showing the importance of macrophages in this context.

Salbutamol Pretreatment Protects the Kidney from bIRI

Thus far, we clarified that *Adrb2* signaling on macrophages plays a critical role in the systemic inflammatory response. Next, we aimed to determine the role of macrophage *Adrb2* signaling in local acute inflammation. For this purpose, we opted to utilize the renal bIRI model, which is generated by 26 minutes of renal ischemia followed by 24 hours of reperfusion.

Vehicle or salbutamol (15 mg/kg) was intraperitoneally administered 24 hours before renal bIRI. Blood and kidney samples were obtained 24 hours after renal bIRI (Figure 4A). Pretreatment with salbutamol provided strong protection from kidney injury as shown by the lower BUN, lower plasma Cre (Figure 4B), and lesser degree of histologic tubular injury (Figure 4, C and D). Thus, systemic pretreatment with salbutamol protects the kidney from bIRI.

Splenic Immune Cells May Play Important Roles in the Protective Effect of Salbutamol against Renal bIRI

Next, we tested whether immune systems were involved in the salbutamol-induced protection against renal bIRI. The spleen is central to the immune system, and splenic immune cell dynamics are thought to be influenced by the degree of sympathetic signaling because the sympathetic nerves are densely distributed in the spleen, as visualized by our tissue

clearing-based 3D immunofluorescence staining of sympathetic nerves (Figure 4E). We conducted a splenectomy 10 days before the bIRI experiment. As a result, the protective effects of salbutamol against renal bIRI were not observed in splenectomized mice (Supplemental Figure 8), suggesting the importance of splenic immune cells in the renoprotective effects of salbutamol.

Macrophage *Adrb2* Signaling Is Critical for the Protective Effect of Salbutamol against Renal bIRI

In order to determine whether macrophages are involved in the salbutamol-induced protection against renal bIRI, we conducted renal bIRI experiments using macrophage-specific *Adrb2* cKO and littermate WT mice (Figure 5A). As a result, deletion of *Adrb2* on macrophages abolished the salbutamol-induced protection against renal bIRI, as shown by the reversal of plasma Cre levels (Figure 5B) and histologic tubular injury scores (Figure 5, C and D). Thus, the protective effects of salbutamol against renal bIRI are primarily due to the activation of *Adrb2* signaling in macrophages.

Adoptive Transfer of Salbutamol-Treated Macrophages Protects the Kidney from bIRI

Given that *Adrb2* signaling on macrophages is critical to protection against kidney injury, we pondered whether *Adrb2* signal-activated macrophages themselves provide protection against renal bIRI and conducted the adoptive transfer experiment (Figure 6A). Adoptive transfer of 1.6×10^5 salbutamol-treated (*Adrb2* signal-activated) macrophages from donor mice protected the kidneys from bIRI in recipient mice, as shown by the lower BUN, lower plasma Cre (Figure 6B), and lesser degree of histologic tubular injury (Figure 6C).

Next, we performed single-cell RNA sequencing (scRNA-seq) of renal tissues to analyze the renoprotective role of salbutamol-treated (*Adrb2* signal-activated) macrophages in detail (Figure 7A). We visualized the single-cell datasets using tSNE and identified 19 cell-type clusters (Figure 7B, Supplemental Table 2). For example, the expression of kidney androgen-regulated protein clearly identified proximal tubular cells in the S3 segment, the most vulnerable sections to ischemic injury (Figure 7B, Supplemental Figure 9A). The violin plot of kidney injury molecule 1 (*Kim1*) expression in this cluster showed that the degree of tubular injury was lower in the bIRI after salbutamol-treated macrophage transfer (Sal_bIRI) condition than in the bIRI after vehicle-treated macrophage transfer (Ctl_bIRI) condition (Figure 7C).

and 136 cells (Sal_bIRI). (D) The violin plot of *Tim3* expressions in the macrophage cluster is drawn. The total numbers of cells in this cluster are as follows: 30 cells (Ctl_sham), 71 cells (Ctl_bIRI), 45 cells (Sal_sham), and 91 cells (Sal_bIRI). *Tim3*-expressing macrophages were accumulated in the injured kidney after salbutamol-treated macrophage transfer (17% [Ctl_sham], 21% [Ctl_bIRI], 4% [Sal_sham], and 33% [Sal_bIRI] of total macrophages in the renal tissue). ATL, ascending thin limb; CD_IC, intercalated cell of the collecting duct; CD_PC, principal cell of the collecting duct; DCT, distal convoluted tubular cell; DTL, descending thin limb; EC, endothelial cell; M ϕ , macrophage; PT (S1/2), proximal tubular cell in the S1/2 segments; PT (S3), proximal tubular cell in the S3 segment; SMC, smooth muscle cell; TAL, thick ascending limb; i.v., intravenous.

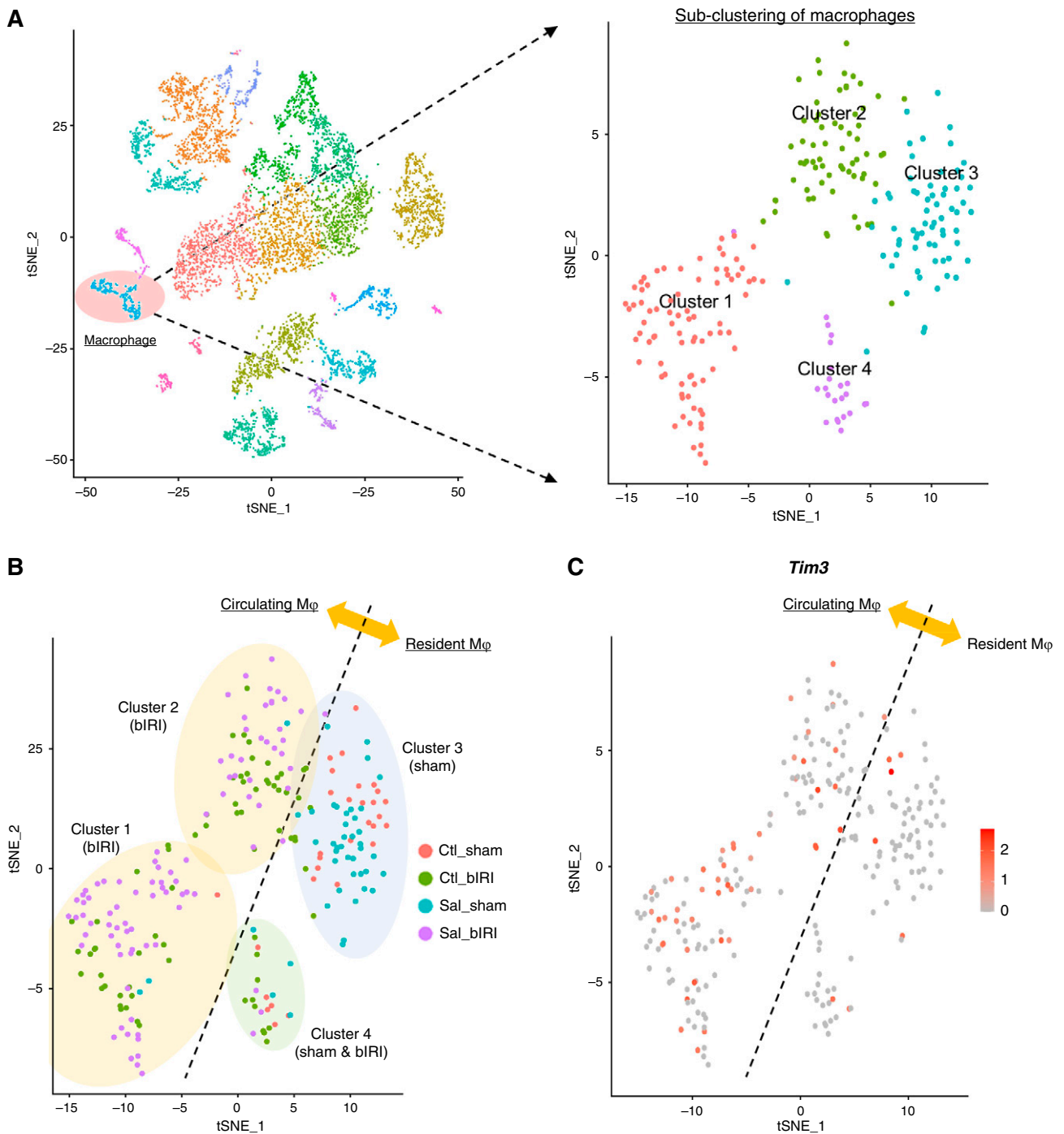


Figure 8. The accumulating *Tim3*-expressing macrophages after bIRI are mainly composed of circulating macrophages. (A) Unbiased subclustering of macrophages is visualized as the tSNE plots. (B) In the tSNE plots with sample information, clusters 1 and 2 are mostly composed of macrophages from bIRI groups (circulating macrophages), whereas cluster 3 is composed of macrophages from sham groups, and cluster 4 contains macrophages from both groups (tissue-resident macrophages). (C) The expression levels of *Tim3* are visualized on the tSNE plots. *Tim3*-expressing macrophages were preferentially distributed on the left side (circulating macrophages). Ctl_bIRI, bilateral ischemia-reperfusion injury after vehicle-treated macrophage transfer; Ctl_sham, sham operation after vehicle-treated macrophage transfer; M ϕ , macrophage; Sal_bIRI, bilateral ischemia-reperfusion injury after salbutamol-treated macrophage transfer; Sal_sham, sham operation after salbutamol-treated macrophage transfer.

We especially focused on *Tim3* expression in the macrophage cluster because high *Tim3* expression is a marker of Adrb2 signal-activated macrophages according to our *in vitro* data (Figure 2). The macrophage cluster was clearly identified in the tSNE plot of single-cell data (Figure 7B) by the expression of two representative markers, *Cd68* and *LysM* (Supplemental Figure 9B). The violin plot of *Tim3* expression in this cluster illustrated that *Tim3*-expressing macrophages (Adrb2 signal-activated macrophages) were particularly accumulated in the renal tissue of the bIRI after salbutamol-treated macrophage transfer condition (Figure 7D), which was also confirmed by immunohistochemistry (Supplemental Figure 10). Furthermore, we investigated the origin of these *Tim3*-expressing macrophages from scRNA-seq data. Unbiased subclustering of macrophages yielded four subclusters (Figure 8A). Clusters 1 and 2 were mostly composed of macrophages from bIRI groups (circulating macrophages), whereas cluster 3 was composed of macrophages from sham groups, and cluster 4 contained macrophages from both groups (tissue-resident macrophages) (Figure 8B). As *Tim3* was preferentially expressed on the left side of the tSNE plots (Figure 8C), the accumulating *Tim3*-expressing macrophages after bIRI might be circulating macrophages. Therefore, Adrb2 signal-activated macrophages with high *Tim3* expression may come from outside the renal tissues and play critical roles in the protection against renal bIRI.

DISCUSSION

In this study, we demonstrated that activation of Adrb2 signaling in macrophages blocks LPS-induced systemic inflammation and protects the kidney from IRI. Furthermore, Adrb2 signaling induces *Tim3* expression, which contributes to anti-inflammatory phenotypic alterations in macrophages.

Adrb2 agonists are known to exert anti-inflammatory effects in several inflammatory diseases, such as LPS-induced sepsis^{3,13} and acute lung injury.¹⁴ However, these *in vivo* observations could not precisely identify the cell type responsible for the anti-inflammatory effect. In our data, the anti-inflammatory effect of salbutamol was mitigated in monocyte-derived macrophage-specific *Adrb2* knockout mice (Figure 3), demonstrating the importance of macrophage Adrb2 signaling in this process. Although sympathetic signaling is known to affect other immune cells, including CD4-positive T cells⁴ and tissue-resident macrophages,^{15,16} our data clearly demonstrated the importance of monocyte-derived macrophages as the critical receiver of sympathetic signaling in LPS-induced systemic inflammation and renal IRI.

Adrb2 signaling has various effects on local inflammation in the kidney (diabetic kidney disease,¹⁷ nephrotoxic injury,¹⁸ and septic kidney injury¹⁹) because adrenergic receptors are ubiquitously expressed in the body. Of note, the Adrb2 agonist formoterol (postinjury administration) was reported to

restore kidney function after renal IRI *via* mitochondrial biogenesis in the proximal tubules.^{20,21} In contrast, we observed the anti-inflammatory effect of salbutamol pretreatment in the acute phase of renal IRI, which was mainly derived from macrophage Adrb2 signaling (Figures 4 and 5, Supplemental Figure 8). The adoptive transfer of Adrb2 signal-activated macrophages also protected the kidney from IRI (Figures 6–8). Taken together, the critical receiver of Adrb2 signaling in renal IRI may differ depending on the timing: Macrophages are important in the acute injury phase, and proximal tubules are important in the recovery phase. Future studies are needed to clarify the interaction between these receivers of Adrb2 signaling and the renal SNS. Prior denervation of renal SNS is known to alleviate the severity of renal IRI in animal studies.²² In contrast, we have previously shown that the renal SNS is denervated after IRI, which results in NE depletion inside the kidney.¹¹ Thus, determination of the influence of renal SNS activity or damage on the dynamics of macrophages and the proximal tubules may aid elucidation of the SNS's role in kidney disease progression.

In this study, we also found that *Tim3* expression was induced by the activation of Adrb2 signaling in macrophages (Figure 2). *Tim3* was included in the 37 genes, which were commonly selected as Adrb2 signal-induced genes from our RNA sequencing data of three *in vitro* macrophage models (Supplemental Table 3). *Tim3* is expressed on many immune cells, including T cells,^{23,24} natural killer cells,²⁵ and dendritic cells,²⁶ and suppresses the immunologic activity as one of the immune checkpoints. Previous studies have shown that *Tim3* is also expressed on macrophages and plays immunosuppressive roles.^{27–30} In our data, *Tim3* knockdown promoted the inflammatory response of macrophages and mitigated the anti-inflammatory effect of salbutamol (Figure 2D, Supplemental Figure 4). In contrast, *Tim3* overexpression attenuated the inflammatory response of macrophages (Supplemental Figure 5). Taken together, these findings indicate that *Tim3* is downstream of Adrb2 signaling and contributes to its anti-inflammatory effect, which cannot be simply explained by the conventional macrophage M1/M2 axis (Supplemental Figure 6). In our scRNA-seq dataset, *Tim3*-expressing macrophages were accumulated in the renal tissue of IRI after the adoptive transfer of Adrb2 signal-activated macrophages (Figure 7D, Supplemental Figure 10), in association with neutrophil's phenotypic change and reduced renal tubular injury (Figure 7C, Supplemental Figure 11–13). Thus, *Tim3*-expressing macrophages induced by Adrb2 signaling may elicit direct protective effects against renal IRI.

Although the mechanism of *Tim3* induction by Adrb2 signaling was not clarified in detail, we at least confirmed that *Tim3* expression induced by Adrb2 activation was dependent on PKA signaling (canonical downstream component of Adrb2 signaling) in macrophages (Figure 2C). As cAMP/PKA signaling is reported to induce promoter/enhancer activity of *Tim3* in Jurkat T cells,³¹ the induction of *Tim3* in

macrophages may also be explained by promoter/enhancer activity.

The spleen is widely innervated by sympathetic nerves, which is also illustrated in our immunofluorescence staining (Figure 4E). Thus, splenic immune cells may be susceptible to sympathetic signaling. In our experiments, prior splenectomy abolished the protective effects of salbutamol against renal IRI (Supplemental Figure 8). In addition, the adoptive transfer of ADRB2 signal-activated splenic macrophages provided strong protection against renal IRI (Figures 6–8). Thus, splenic macrophages may play important roles in the anti-inflammatory effects of systemic salbutamol administration. The critical role of the spleen in neuroimmune interactions was also reported in the cholinergic anti-inflammatory pathway.^{32–35} The cholinergic anti-inflammatory pathway, which is activated by electrical stimulation of the vagus nerve, is mediated by the spleen.^{36–38} Vagus nerve induces the activation of splenic sympathetic nerves, leading to the NE-induced activation of CD4-positive T cells in the spleen.^{39–41} Various types of splenic immune cells, including macrophages and T cells, may interact with one another and alter the immunologic dynamics in responding to sympathetic signaling. Further studies using single-cell analysis are needed to elucidate the immunologic dynamics in the spleen in response to splenic SNS activation.

Finally, it is important to determine whether the anti-inflammatory role of ADRB2 signaling can be applied in clinical treatment for inflammatory diseases. In our study, ADRB2 activation induced an anti-inflammatory response in differentiated U937 cells (human macrophages) as well as mouse macrophages (Figure 1, Supplemental Figure 2), suggesting that our concept can be applied to human inflammatory diseases. Indeed, genetic variation of *ADRB2* was associated with increased mortality and more organ dysfunction in septic shock in a clinical study.⁴² However, a multicenter, randomized controlled trial (BALTI-2) failed to show the benefits of intravenous salbutamol treatment in the course of acute respiratory distress syndrome.⁴³ In this previous study, salbutamol treatment was poorly tolerated due to the problem of hemodynamics, including tachycardia and arrhythmia.⁴³ Thus, cell type-specific activation of ADRB2 signaling may be needed to prevent such cardiac side effects. In our data, macrophages were the critical receiver of ADRB2 signaling in the protection against renal IRI. As demonstrated in our experiment (Figures 6–8), the adoptive transfer of ADRB2 signal-activated immune cells is a promising candidate for clinical application, although infection risks during immune cell harvest and treatment cannot be ignored in the clinical setting.

Our study has several limitations. First, the scRNA-seq data in our study lacked sufficient statistical power with respect to the dispersion of *Kim1* expression in proximal tubules and *Tim3* expression in macrophages in the renal tissues (Figure 7). Although we need to increase kidney samples to make a conclusion by the scRNA-seq data alone, the results were compatible with *in vitro* and *in vivo* data in the rest of our study,

providing the potential mechanism for the protection against renal IRI induced by the adoptive transfer of salbutamol-treated macrophages. Second, our study did not examine how the ADRB2 signal-activated macrophages affect other immune cell dynamics, such as T cells, B cells, natural killer cells, and dendritic cells. The renoprotective effect of the adoptive transfer of salbutamol-treated macrophages might be partially induced by the interaction with other immune cells. The analysis of immune cell dynamics in the lymphoid tissues after the adoptive transfer of ADRB2 signal-activated macrophages would provide additional insights concerning the role of macrophages in the whole immune dynamics.

In conclusion, the activation of ADRB2 signaling in macrophages induces anti-inflammatory phenotypic alterations partially via the induction of *Tim3* expression, which blocks LPS-induced systemic inflammation and protects against renal IRI. Our data provide important insights concerning neuroimmune interactions in the pathophysiology of inflammatory diseases.

DISCLOSURES

The Division of CKD Pathophysiology, University of Tokyo is financially supported by Kyowa Kirin Co. Ltd. R. Inagi reports research funding from Kyowa Kirin Co. Ltd. and Nipro; honoraria from Alexion, Bayer, Chugai, Kyowa Kirin Co. Ltd., Mitsubishi Tanabe, MSD, Research and Development Support Center, Kowa, and Sumitomo Dainippon; scientific advisor or membership as associate editor of *Clinical and Experimental Pharmacology Physiology* and *K360* and as editorial board member of *American Journal of Physiology Renal Physiology*, *Kidney International*, and *Kidney Research and Clinical Practice*; and other interests/relationships as councilor and secretary of the Japanese Society of Nephrology (international liaison committee) and the International Maillard Reaction Society (IMARS; chief editor of *IMARS Highlights*). I. Komuro reports research funding from AstraZeneca, Japan, Astellas Pharma Inc., Bayer Yakuin, Ltd., Daiichi Sankyo Company, Limited, Kowa Pharmaceutical Co. Ltd., Mitsubishi Tanabe Pharma Corporation, ONO PHARMACEUTICAL CO., LTD., Otsuka Pharmaceutical Co., Ltd., Sanofi, K.K., Sumitomo Dainippon Pharma Co., Ltd., Takeda Pharmaceutical Company Limited, and Teijin Pharma Limited and honoraria from AstraZeneca, Japan, Daiichi Sankyo Company, Limited, Mitsubishi Tanabe Pharma Corporation, ONO PHARMACEUTICAL CO., LTD., and Takeda Pharmaceutical Company Limited. M. Nangaku reports honoraria from AstraZeneca and Boehringer Ingelheim and scientific advisor or membership with Akebia, Astellas, Bayer, Boehringer-Ingelheim, Daiichi-Sankyo, GlaxoSmithKline, Japan Tobacco Inc., Kyowa Kirin Co. Ltd., and Mitsubishi-Tanabe. E. A. Susaki and H. R. Ueda are coinventors of patents owned by RIKEN. E. A. Susaki reports patents and inventions with Tokyo Chemical Industry, CO, LTD; speakers bureau with Tokyo Chemical Industry, CO, LTD; and other interests/relationships as a senior researcher at CUBICStars Co. H. R. Ueda reports ownership interest in CUBICStars Inc.; research funding from Olympus Corporation; and patents and inventions with CUBICStars Inc. (inventions on CUBIC-HV reagents) and RIKEN (inventions on CUBIC reagents). All remaining authors have nothing to disclose.

FUNDING

This work was supported by Japan Society for the Promotion of Science (JSPS) Grant-in-Aid for Japan Society for JSPS Research Fellow JSPS

KAKENHI grant 19J11928 (to S. Hasegawa); MSD Life Science Foundation (S. Hasegawa and T. Inoue); Japan Society for the Promotion of Science Grant-in-Aid for Scientific Research (B) JSPS KAKENHI grants 18H02727 (to R. Inagi) and 18H02824 (to M. Nangaku); Kyowa Kirin Co. Ltd. (R. Inagi); Japan Agency for Medical Research and Development grants JP20gm6210013 (to T. Inoue) and JP20gm6210010 (to S. Nomura); Japan Society for the Promotion of Science Grant-in-Aid for Research Activity Start-Up and for Young Scientists JSPS KAKENHI grants 18H06192 (to T. Inoue) and 20K17242 (to T. Inoue); Kidney Foundation grant JKFB18-3 (to T. Inoue); Salt Science Research Foundation grant 1919 (to T. Inoue); Smoking Research Foundation (to T. Inoue); Yukiko Ishibashi Foundation (to T. Inoue); Mochida Memorial Foundation (to T. Inoue); Takeda Science Foundation (to T. Inoue); Astellas Foundation for Research on Metabolic Disorders (to T. Inoue); and Suzuken Memorial Foundation (to T. Inoue). This work was partially carried out under the support of Isotope Science Center, University of Tokyo. Part of this study was performed in collaboration with Olympus Corporation and with kind software support by Bitplane.

ACKNOWLEDGMENTS

The authors are grateful to Dr. Naoki Kuramoto, Dr. Yu Hirata, Prof. Wataru Ogawa (Kobe University), and Prof. Gerard Karsenty (Columbia University) for providing the *Adrb2 flox* mice. The authors also thank Ms. Ikumi Okuaki, Ms. Rieko Matsuda, Ms. Kahoru Amitani, Ms. Sayaka Hayashi, and Ms. Nanako Shida for their technical support. The illustrations of mice, kidneys, and petri dishes were obtained from TogoTV (2016 DBCLS TogoTV).

Sho Hasegawa performed the main experiments, analyzed the data, and wrote the original draft; Nobuyoshi Akimitsu, Rie Fujii, Daichi Fukaya, Tsuyoshi Inoue, Yasuna Nakamura, Atsuko Nakanishi Ozeki, Wachirasek Peerapanyasut, Rie Uni, and Chia-Hsien Wu performed or contributed to the animal experiments; Takahide Kohro, Akashi Taguchi, and Youichiro Wada performed the HiSeq2500 run and data processing in the RNA sequencing analysis; Mikako Katagiri, Toshiyuki Ko, Issei Komuro, Seitaro Nomura, and Shintaro Yamada aided our scRNA-seq analysis; Etsuo A. Susaki and Hiroki R. Ueda aided 3D visualization using tissue clearing; Reiko Inagi, Tsuyoshi Inoue, and Masaomi Nangaku supervised this study and revised the manuscript; and all authors approved the final version of the manuscript.

SUPPLEMENTAL MATERIAL

This article contains the following supplemental material online at <http://jasn.asnjournals.org/lookup/suppl/doi:10.1681/ASN.2020121723/-/DCSupplemental>.

Supplemental Figure 1. The effect of β 2-adrenergic receptor signaling on various inflammatory cytokines.

Supplemental Figure 2. The anti-inflammatory effect of β 2-adrenergic receptor signaling is common in macrophages of various origins.

Supplemental Figure 3. The detailed protocols of RNA sequencing experiments.

Supplemental Figure 4. The effect of T cell Ig and mucin domain 3 knock-down using another small interfering RNA on the inflammatory response of macrophages.

Supplemental Figure 5. The effect of T cell Ig and mucin domain 3 overexpression on the inflammatory response of macrophages.

Supplemental Figure 6. The effect of β 2-adrenergic receptor signaling on macrophage M1/M2 markers.

Supplemental Figure 7. Assessment of renal damage in the LPS-induced septic model.

Supplemental Figure 8. Prior splenectomy abolishes the protective effect of salbutamol pretreatment against renal ischemia-reperfusion injury.

Supplemental Figure 9. Cell-type marker gene expression levels for unbiased clustering of single-cell RNA sequencing data.

Supplemental Figure 10. Immunostaining of T cell Ig and mucin domain 3 on renal tissues of the adoptive transfer experiment.

Supplemental Figure 11. Assessment of infiltrating neutrophils in the single-cell RNA sequencing data.

Supplemental Figure 12. M1/M2 marker gene expression levels on the macrophage subclustering data in the single-cell RNA sequencing.

Supplemental Figure 13. The adoptive transfer of salbutamol-treated macrophages 2 days before renal ischemia-reperfusion injury does not provide protection.

Supplemental Table 1. Primer sequences for the quantitative real-time PCRs.

Supplemental Table 2. A list of the marker genes of each cluster in the single-cell RNA sequencing.

Supplemental Table 3. A list of the 37 genes commonly selected in the RNA sequencing from the three *in vitro* models.

REFERENCES

1. Felten DL, Felten SY, Carlson SL, Olschowka JA, Livnat S: Noradrenergic and peptidergic innervation of lymphoid tissue. *J Immunol* 135[Suppl]: 755s–765s, 1985
2. Nance DM, Sanders VM: Autonomic innervation and regulation of the immune system (1987–2007). *Brain Behav Immun* 21: 736–745, 2007
3. Ağaç D, Estrada LD, Maples R, Hooper LV, Farrar JD: The β 2-adrenergic receptor controls inflammation by driving rapid IL-10 secretion. *Brain Behav Immun* 74: 176–185, 2018
4. Araujo LP, Maricato JT, Guerreschi MG, Takenaka MC, Nascimento VM, de Melo FM, et al.: The sympathetic nervous system mitigates CNS autoimmunity via β 2-adrenergic receptor signaling in immune cells. *Cell Rep* 28: 3120–3130.e5, 2019
5. Nakai A, Hayano Y, Furuta F, Noda M, Suzuki K: Control of lymphocyte egress from lymph nodes through β 2-adrenergic receptors. *J Exp Med* 211: 2583–2598, 2014
6. Arima Y, Harada M, Kamimura D, Park JH, Kawano F, Yull FE, et al.: Regional neural activation defines a gateway for autoreactive T cells to cross the blood-brain barrier. *Cell* 148: 447–457, 2012
7. Hinoi E, Gao N, Jung DY, Yadav V, Yoshizawa T, Myers MG Jr, et al.: The sympathetic tone mediates leptin's inhibition of insulin secretion by modulating osteocalcin bioactivity. *J Cell Biol* 183: 1235–1242, 2008
8. Susaki EA, Tainaka K, Perrin D, Kishino F, Tawara T, Watanabe TM, et al.: Whole-brain imaging with single-cell resolution using chemical cocktails and computational analysis. *Cell* 157: 726–739, 2014
9. Kubota SI, Takahashi K, Nishida J, Morishita Y, Ehata S, Tainaka K, et al.: Whole-body profiling of cancer metastasis with single-cell resolution. *Cell Rep* 20: 236–250, 2017
10. Tainaka K, Murakami TC, Susaki EA, Shimizu C, Saito R, Takahashi K, et al.: Chemical landscape for tissue clearing based on hydrophilic reagents. *Cell Rep* 24: 2196–2210.e9, 2018
11. Hasegawa S, Susaki EA, Tanaka T, Komaba H, Wada T, Fukagawa M, et al.: Comprehensive three-dimensional analysis (CUBIC-kidney) visualizes abnormal renal sympathetic nerves after ischemia/reperfusion injury. *Kidney Int* 96: 129–138, 2019
12. Hasegawa S, Tanaka T, Saito T, Fukui K, Wakashima T, Susaki EA, et al.: The oral hypoxia-inducible factor prolyl hydroxylase inhibitor enarodustat counteracts alterations in renal energy metabolism in the early stages of diabetic kidney disease. *Kidney Int* 97: 934–950, 2020
13. Nakamura A, Imaizumi A, Yanagawa Y, Kohsaka T, Johns EJ: β 2-Adrenoceptor activation attenuates endotoxin-induced acute renal failure. *J Am Soc Nephrol* 15: 316–325, 2004
14. Grailer JJ, Haggadone MD, Sarma JV, Zetoune FS, Ward PA: Induction of M2 regulatory macrophages through the β 2-adrenergic receptor

- with protection during endotoxemia and acute lung injury. *J Innate Immun* 6: 607–618, 2014
15. Tang L, Okamoto S, Shiuchi T, Toda C, Takagi K, Sato T, et al.: Sympathetic nerve activity maintains an anti-inflammatory state in adipose tissue in male mice by inhibiting TNF- α gene expression in macrophages. *Endocrinology* 156: 3680–3694, 2015
 16. Gabanyi I, Muller PA, Feighery L, Oliveira TY, Costa-Pinto FA, Mucida D: Neuro-immune interactions drive tissue programming in intestinal macrophages. *Cell* 164: 378–391, 2016
 17. Noh H, Yu MR, Kim HJ, Lee JH, Park BW, Wu IH, et al.: Beta 2-adrenergic receptor agonists are novel regulators of macrophage activation in diabetic renal and cardiovascular complications. *Kidney Int* 92: 101–113, 2017
 18. Arif E, Solanki AK, Srivastava P, Rahman B, Fitzgibbon WR, Deng P, et al.: Mitochondrial biogenesis induced by the β 2-adrenergic receptor agonist formoterol accelerates podocyte recovery from glomerular injury. *Kidney Int* 96: 656–673, 2019
 19. Nakamura A, Niimi R, Yanagawa Y: Protection from sepsis-induced acute renal failure by adenoviral-mediated gene transfer of beta2-adrenoceptor. *Nephrol Dial Transplant* 25: 730–737, 2010
 20. Jesinkey SR, Funk JA, Stallons LJ, Wills LP, Megyesi JK, Beeson CC, et al.: Formoterol restores mitochondrial and renal function after ischemia-reperfusion injury. *J Am Soc Nephrol* 25: 1157–1162, 2014
 21. Cameron RB, Gibbs WS, Miller SR, Dupre TV, Megyesi J, Beeson CC, et al.: Proximal tubule β 2-adrenergic receptor mediates formoterol-induced recovery of mitochondrial and renal function after ischemia-reperfusion injury. *J Pharmacol Exp Ther* 369: 173–180, 2019
 22. Fujii T, Kurata H, Takaoka M, Muraoka T, Fujisawa Y, Shokoji T, et al.: The role of renal sympathetic nervous system in the pathogenesis of ischemic acute renal failure. *Eur J Pharmacol* 481: 241–248, 2003
 23. Gautron AS, Dominguez-Villar M, de Marcken M, Hafler DA: Enhanced suppressor function of TIM-3+ FoxP3+ regulatory T cells. *Eur J Immunol* 44: 2703–2711, 2014
 24. Anderson AC, Joller N, Kuchroo VK: Lag-3, Tim-3, and TIGIT: Co-inhibitory receptors with specialized functions in immune regulation. *Immunity* 44: 989–1004, 2016
 25. da Silva IP, Gallois A, Jimenez-Baranda S, Khan S, Anderson AC, Kuchroo VK, et al.: Reversal of NK-cell exhaustion in advanced melanoma by Tim-3 blockade. *Cancer Immunol Res* 2: 410–422, 2014
 26. Chiba S, Baghdadi M, Akiba H, Yoshiyama H, Kinoshita I, Dosaka-Akita H, et al.: Tumor-infiltrating DCs suppress nucleic acid-mediated innate immune responses through interactions between the receptor TIM-3 and the alarmin HMGB1. *Nat Immunol* 13: 832–842, 2012
 27. Yang X, Jiang X, Chen G, Xiao Y, Geng S, Kang C, et al.: T cell Ig mucin-3 promotes homeostasis of sepsis by negatively regulating the TLR response. *J Immunol* 190: 2068–2079, 2013
 28. Ocaña-Guzman R, Torre-Bouscoulet L, Sada-Ovalle I: TIM-3 regulates distinct functions in macrophages. *Front Immunol* 7: 229, 2016
 29. Li ZH, Wang LL, Liu H, Muyayalo KP, Huang XB, Mor G, et al.: Galectin-9 alleviates LPS-induced preeclampsia-like impairment in rats via switching decidual macrophage polarization to M2 subtype. *Front Immunol* 9: 3142, 2019
 30. Liang S, Cai J, Li Y, Yang R: 1,25-Dihydroxy-Vitamin D3 induces macrophage polarization to M2 by upregulating T-cell Ig-mucin-3 expression. *Mol Med Rep* 19: 3707–3713, 2019
 31. Yun SJ, Lee B, Komori K, Lee MJ, Lee BG, Kim K, et al.: Regulation of TIM-3 expression in a human T cell line by tumor-conditioned media and cyclic AMP-dependent signaling. *Mol Immunol* 105: 224–232, 2019
 32. Borovikova LV, Ivanova S, Zhang M, Yang H, Botchkina GI, Watkins LR, et al.: Vagus nerve stimulation attenuates the systemic inflammatory response to endotoxin. *Nature* 405: 458–462, 2000
 33. Wang H, Yu M, Ochani M, Amella CA, Tanovic M, Susarla S, et al.: Nicotinic acetylcholine receptor alpha7 subunit is an essential regulator of inflammation. *Nature* 421: 384–388, 2003
 34. Pavlov VA, Tracey KJ: Neural regulation of immunity: Molecular mechanisms and clinical translation. *Nat Neurosci* 20: 156–166, 2017
 35. Tracey KJ: Reflex control of immunity. *Nat Rev Immunol* 9: 418–428, 2009
 36. Huston JM, Ochani M, Rosas-Ballina M, Liao H, Ochani K, Pavlov VA, et al.: Splenectomy inactivates the cholinergic antiinflammatory pathway during lethal endotoxemia and polymicrobial sepsis. *J Exp Med* 203: 1623–1628, 2006
 37. Inoue T, Abe C, Sung SS, Moscalu S, Jankowski J, Huang L, et al.: Vagus nerve stimulation mediates protection from kidney ischemia-reperfusion injury through α 7nAChR+ splenocytes. *J Clin Invest* 126: 1939–1952, 2016
 38. Abe C, Inoue T, Inglis MA, Viar KE, Huang L, Ye H, et al.: C1 neurons mediate a stress-induced anti-inflammatory reflex in mice. *Nat Neurosci* 20: 700–707, 2017
 39. Rosas-Ballina M, Olofsson PS, Ochani M, Valdés-Ferrer SI, Levine YA, Reardon C, et al.: Acetylcholine-synthesizing T cells relay neural signals in a vagus nerve circuit. *Science* 334: 98–101, 2011
 40. Inoue T, Abe C, Kohro T, Tanaka S, Huang L, Yao J, et al.: Non-canonical cholinergic anti-inflammatory pathway-mediated activation of peritoneal macrophages induces Hes1 and blocks ischemia/reperfusion injury in the kidney. *Kidney Int* 95: 563–576, 2019
 41. Hasegawa S, Inoue T, Inagi R: Neuroimmune interactions and kidney disease. *Kidney Res Clin Pract* 38: 282–294, 2019
 42. Nakada TA, Russell JA, Boyd JH, Aguirre-Hernandez R, Thain KR, Thair SA, et al.: beta2-Adrenergic receptor gene polymorphism is associated with mortality in septic shock. *Am J Respir Crit Care Med* 181: 143–149, 2010
 43. Gao Smith F, Perkins GD, Gates S, Young D, McAuley DF, Tunnicliffe W, et al.; BALTI-2 study investigators: Effect of intravenous β -2 agonist treatment on clinical outcomes in acute respiratory distress syndrome (BALTI-2): A multicentre, randomised controlled trial. *Lancet* 379: 229–235, 2012

AFFILIATIONS

¹Division of Nephrology and Endocrinology, University of Tokyo Graduate School of Medicine, Tokyo, Japan

²Division of CKD Pathophysiology, University of Tokyo Graduate School of Medicine, Tokyo, Japan

³Department of Physiology of Visceral Function and Body Fluid, Nagasaki University Graduate School of Biomedical Sciences, Nagasaki, Japan

⁴Department of Nephrology, Saitama Medical University, Saitama, Japan

⁵Mahidol University, Nakhonsawan Campus, Nakhonsawan, Thailand

⁶Isotope Science Center, University of Tokyo, Tokyo, Japan

⁷Department of Clinical Informatics/Cardiology, Jichi Medical University, Tochigi, Japan

⁸Department of Cardiovascular Medicine, University of Tokyo Graduate School of Medicine, Tokyo, Japan

⁹Genome Science Division, Research Center for Advanced Science and Technologies, University of Tokyo, Tokyo, Japan

¹⁰Department of Systems Pharmacology, The University of Tokyo Graduate School of Medicine, Tokyo, Japan

¹¹Laboratory for Synthetic Biology, RIKEN Center for Biosystems Dynamics Research, Suita, Japan

Supplemental materials for

Activation of sympathetic signaling in macrophages blocks systemic inflammation and protects against renal ischemia/reperfusion injury

Table of Contents

Supplemental Figure 1. The effect of β 2-adrenergic receptor signaling on various inflammatory cytokines

Supplemental Figure 2. The anti-inflammatory effect of β 2-adrenergic receptor signaling is common in macrophages of various origins

Supplemental Figure 3. The detailed protocols of RNA sequencing experiments

Supplemental Figure 4. The effect of T-cell immunoglobulin and mucin domain 3 knockdown using another small interfering RNA on the inflammatory response of macrophages

Supplemental Figure 5. The effect of T-cell immunoglobulin and mucin domain 3 overexpression on the inflammatory response of macrophages

Supplemental Figure 6. The effect of β 2-adrenergic receptor signaling on macrophage M1/M2 markers

Supplemental Figure 7. Assessment of renal damage in the lipopolysaccharide-induced septic model

Supplemental Figure 8. Prior splenectomy abolishes the protective effect of salbutamol pretreatment against renal ischemia/reperfusion injury

Supplemental Figure 9. Cell-type marker gene expression levels for unbiased clustering of single-cell RNA sequencing data

Supplemental Figure 10. Immunostaining of T-cell immunoglobulin and mucin

domain 3 on renal tissues of the adoptive transfer experiment

Supplemental Figure 11. Assessment of infiltrating neutrophils in the single-cell RNA sequencing data

Supplemental Figure 12. M1/M2 marker gene expression levels on the macrophage sub-clustering data in the single-cell RNA sequencing

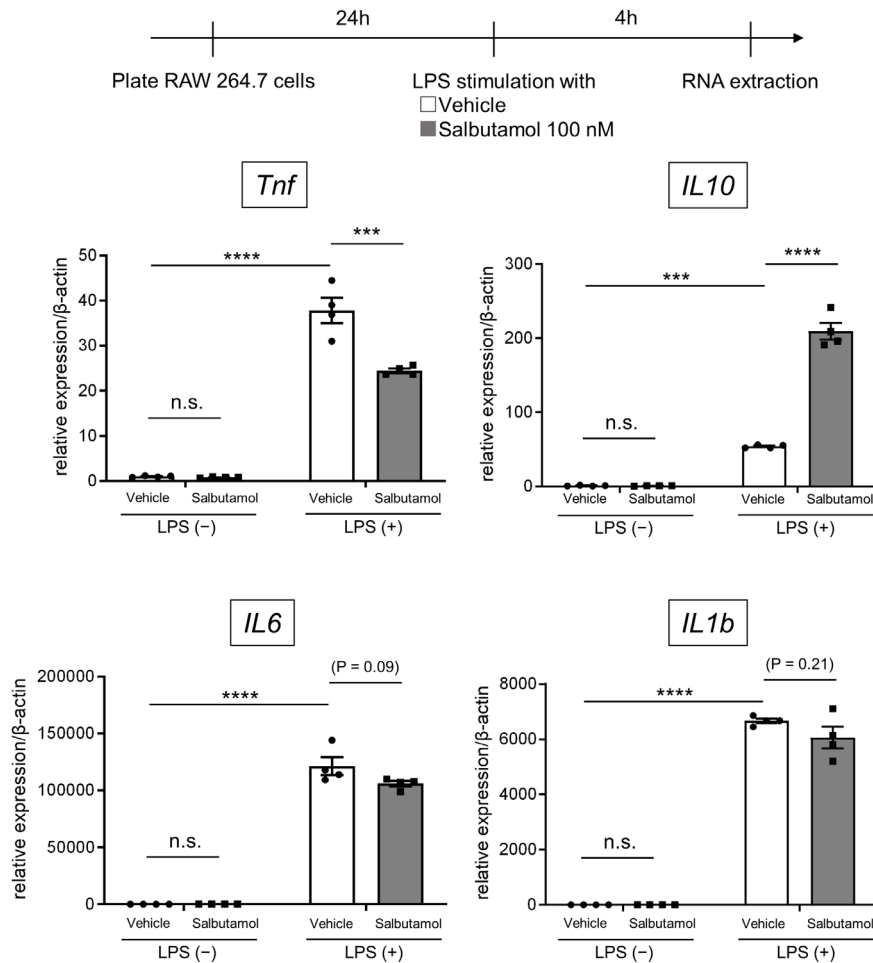
Supplemental Figure 13. The adoptive transfer of salbutamol-treated macrophages two days before renal ischemia/reperfusion injury does not provide protection

Supplemental Table 1. Primer sequences for the quantitative real-time polymerase chain reactions

Supplemental Table 2. A list of the marker genes of each cluster in the single-cell RNA sequencing

Supplemental Table 3. A list of the 37 genes commonly selected in the RNA sequencing from the three *in vitro* models

Supplemental Figure 1

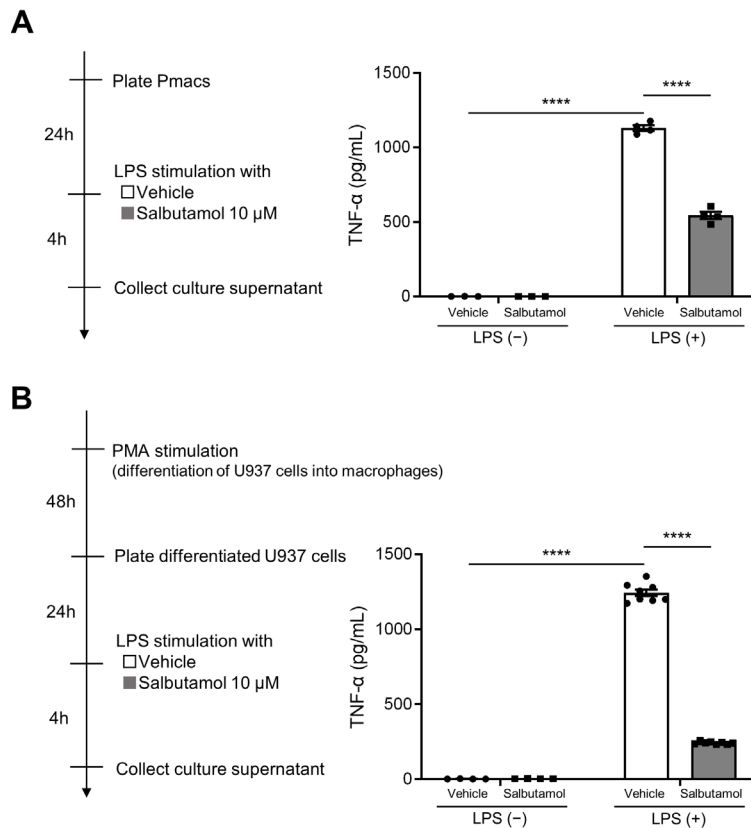


Supplemental Figure 1. The effect of β 2-adrenergic receptor signaling on various inflammatory cytokines

The expressions of pro-inflammatory cytokines such as tumor necrosis factor (*Tnf*), interleukin 6 (*IL6*) and interleukin 1 beta (*IL1b*) tended to be suppressed, whereas the expression of interleukin 10 (*IL10*), an anti-inflammatory cytokine, was upregulated by the salbutamol treatment (n = 4).

All data are presented as means \pm standard error of the mean. Statistical comparisons were analyzed by a two-way analysis of variance with a *post hoc* Tukey's multiple comparisons test. ****P < 0.001, *****P < 0.0001, n.s.; not significant.

Supplemental Figure 2



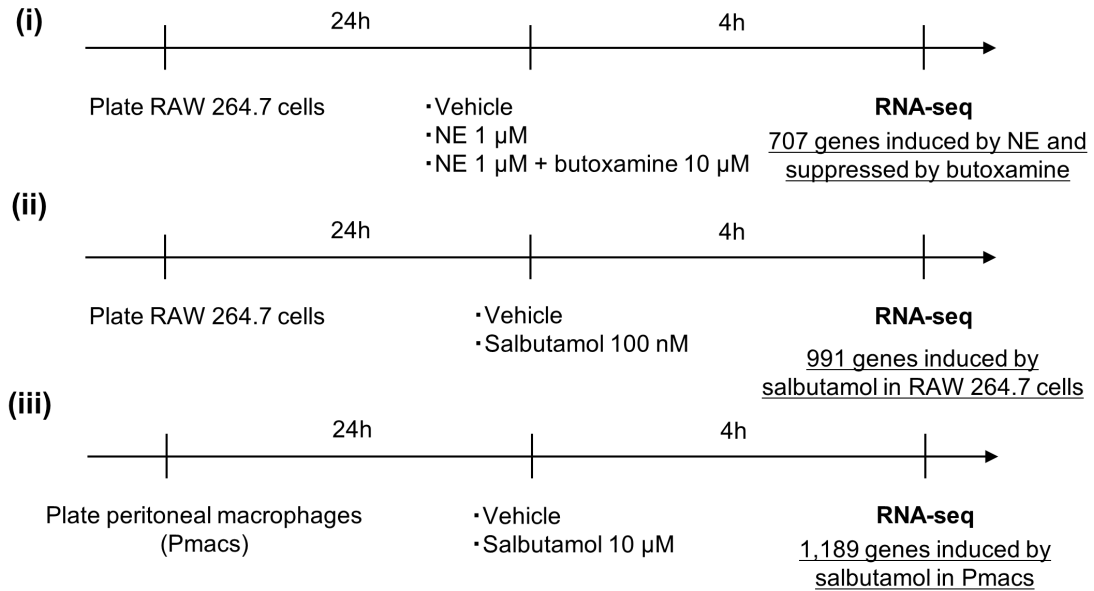
Supplemental Figure 2. The anti-inflammatory effect of β 2-adrenergic receptor signaling is common in macrophages of various origins

(A) Salbutamol, a selective β 2-adrenergic receptor agonist, suppressed tumor necrosis factor- α (TNF- α) induction by lipopolysaccharide (LPS) in peritoneal macrophages (Pmacs) (n = 3-4).

(B) U937 cells (human monocyte cell line) were differentiated into macrophages by phorbol 12-myristate 13-acetate (PMA) stimulation. Salbutamol suppressed TNF- α induction by LPS in human macrophages (n = 4 or 8).

All data are presented as means \pm standard error of the mean. Statistical comparisons were analyzed by a two-way analysis of variance with a *post hoc* Tukey's multiple comparisons test. ****P < 0.0001.

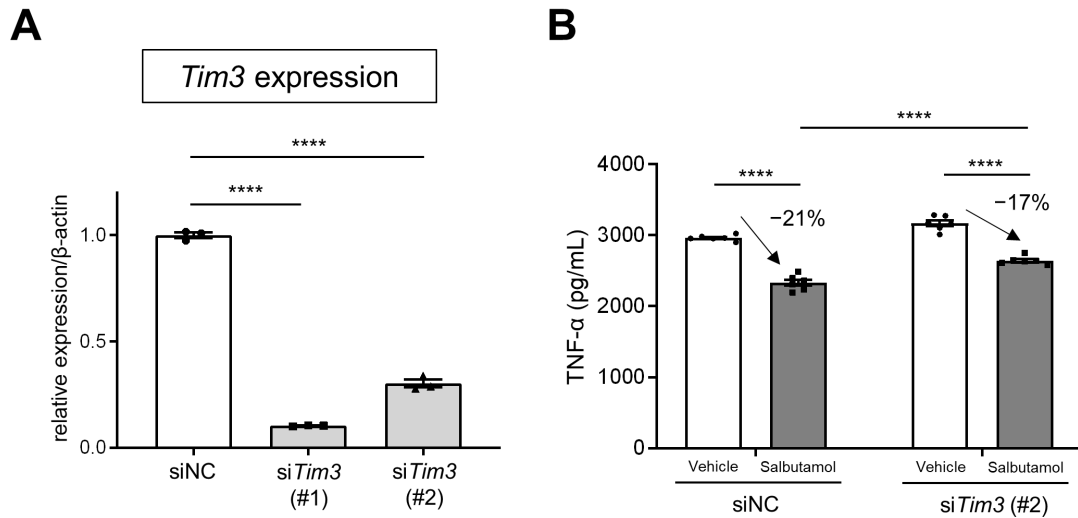
Supplemental Figure 3



Supplemental Figure 3. The detailed protocols of RNA sequencing experiments

RNA sequencing (RNA-seq) was conducted for three different *in vitro* macrophage-models. β 2-adrenergic receptor signaling-induced genes were respectively selected in each model ([i] 707 genes, [ii] 991 genes and [iii] 1,189 genes).

Supplemental Figure 4



Supplemental Figure 4. The effect of T-cell immunoglobulin and mucin domain 3 knockdown using another small interfering RNA on the inflammatory response of macrophages

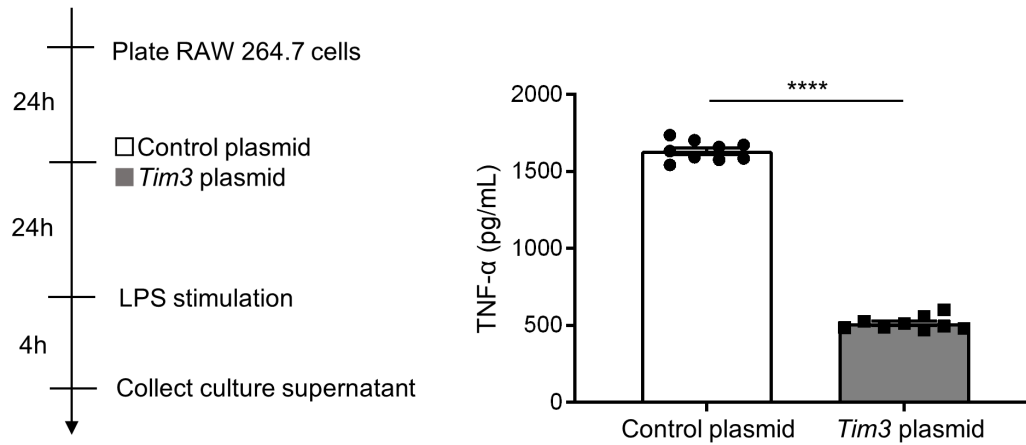
(A) Quantitative real-time polymerase chain reaction confirmed the efficient knockdown of T-cell immunoglobulin and mucin domain 3 (*Tim3*) by small interfering RNA (siRNA). si*Tim3* (#1) was used in Figure 2D and si*Tim3* (#2) was used in Supplemental Figure 4B (n = 3).

(B) The same experiment as Figure 2D was performed using si*Tim3* (#2) (n = 6).

All data are presented as means \pm standard error of the mean. For multiplex comparisons, a one-way analysis of variance (ANOVA) (A) or two-way ANOVA (B) with a *post hoc* Tukey's multiple comparisons test was applied. ****P < 0.0001.

TNF- α , tumor necrosis factor- α .

Supplemental Figure 5



Supplemental Figure 5. The effect of T-cell immunoglobulin and mucin domain 3 overexpression on the inflammatory response of macrophages

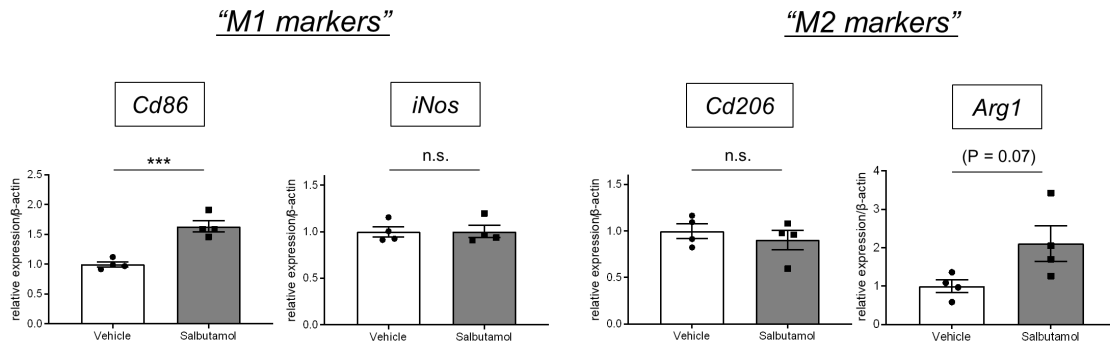
T-cell immunoglobulin and mucin domain 3 (*Tim3*) overexpression suppressed the inflammatory response of RAW 264.7 cells (n = 9).

Data are presented as means \pm standard error of the mean. The statistical comparison was analyzed by an unpaired two-tailed *t* test. ****P < 0.0001.

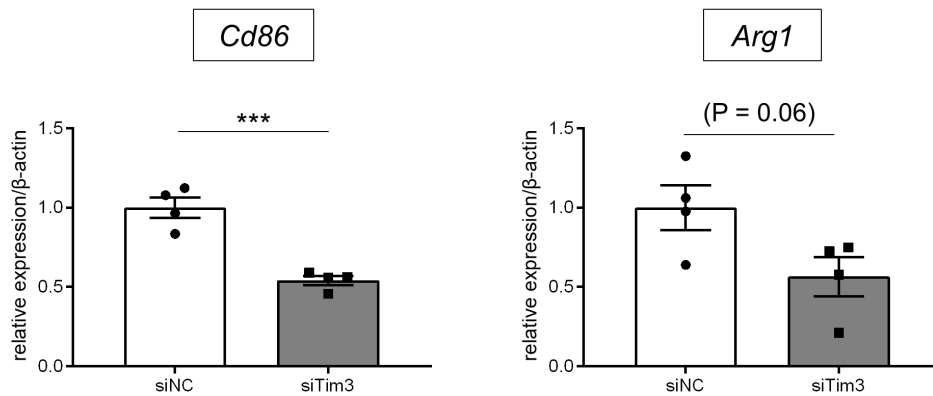
LPS, lipopolysaccharide; TNF- α , tumor necrosis factor- α .

Supplemental Figure 6

A



B

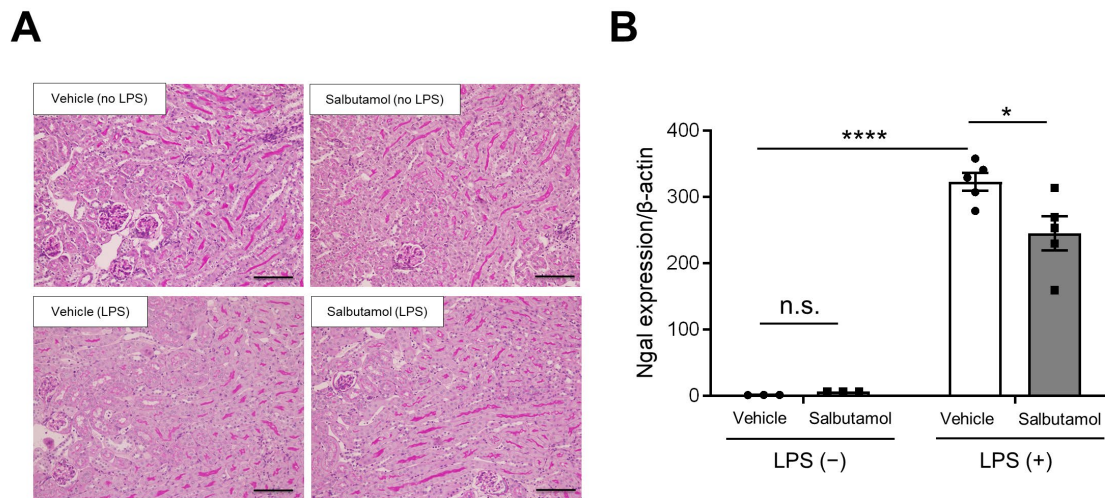


Supplemental Figure 6. The effect of β₂-adrenergic receptor signaling on macrophage M1/M2 markers

β₂-adrenergic receptor (*Adrb2*) signal-induced phenotypic alterations in macrophages could not be straightforwardly explained by the conventional M1/M2 axis because salbutamol treatment (100 nM) upregulated the expressions of M1 marker *Cd86* as well as M2 marker arginase 1 (*Arg1*). T-cell immunoglobulin and mucin domain 3 (*Tim3*) knockdown showed the opposite effects on these M1/M2 markers.

All data are presented as means ± standard error of the mean. Statistical comparisons were analyzed by an unpaired two-tailed *t* test. ***P < 0.001, n.s.; not significant.

Supplemental Figure 7



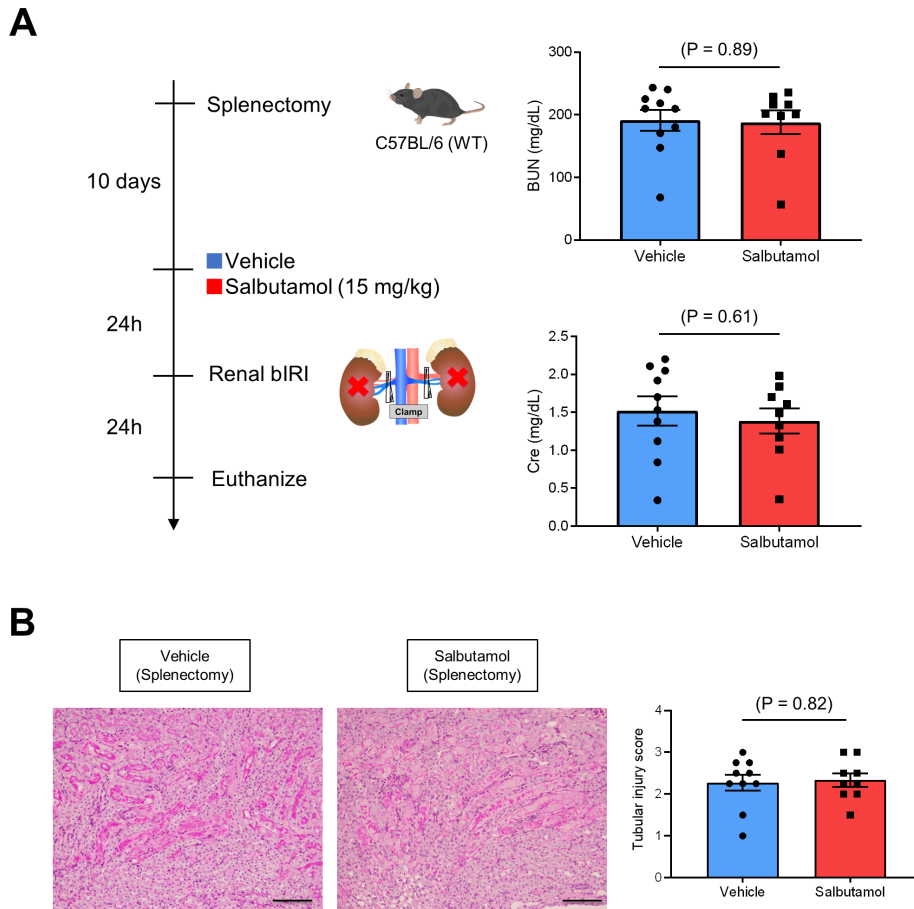
Supplemental Figure 7. Assessment of renal damage in the lipopolysaccharide-induced septic model

(A) Representative Periodic acid-Schiff staining of the renal tissues in Figure 3A is shown. Renal histological injury was not observed 4h after lipopolysaccharide (LPS) administration. Scale bar = 100 μ m.

(B) The expression of neutrophil gelatinase-associated lipocalin (*Ngal*) in the renal tissues 4h after LPS administration was significantly suppressed in the salbutamol-treated group compared with vehicle-treated group (n = 3 or 5).

Data are presented as means \pm standard error of the mean. The statistical comparison was analyzed by a two-way analysis of variance with a *post hoc* Tukey's multiple comparisons test. *P < 0.05, ****P < 0.0001, n.s.; not significant.

Supplemental Figure 8

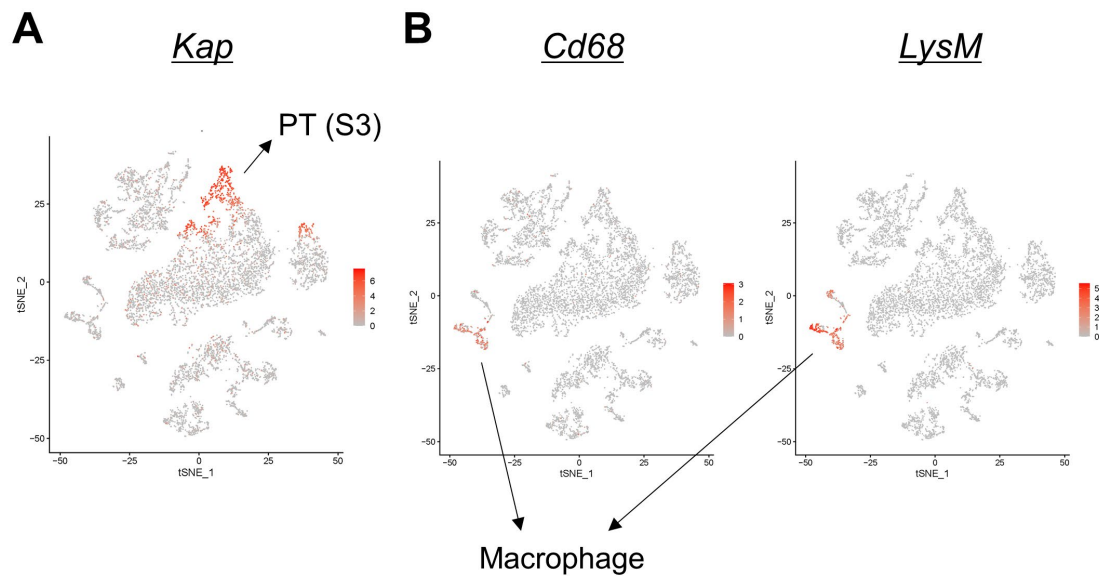


Supplemental Figure 8. Prior splenectomy abolishes the protective effect of salbutamol pretreatment against renal ischemia/reperfusion injury

(A) Vehicle or salbutamol was intraperitoneally administered to splenectomized mice 24 h before renal bilateral ischemia/reperfusion injury (bIRI). Blood and kidney samples were obtained 24 h after bIRI. The blood urea nitrogen (BUN) and plasma creatinine (Cre) levels did not differ between the vehicle and salbutamol groups ($n = 9-10$).

(B) Representative Periodic acid-Schiff staining of the renal outer medulla is shown on the left side (Scale bar = 100 μ m). The histological tubular injury scores did not differ between groups ($n = 9-10$). All data are presented as means \pm standard error of the mean. Statistical comparisons were analyzed by an unpaired two-tailed t test.

Supplemental Figure 9

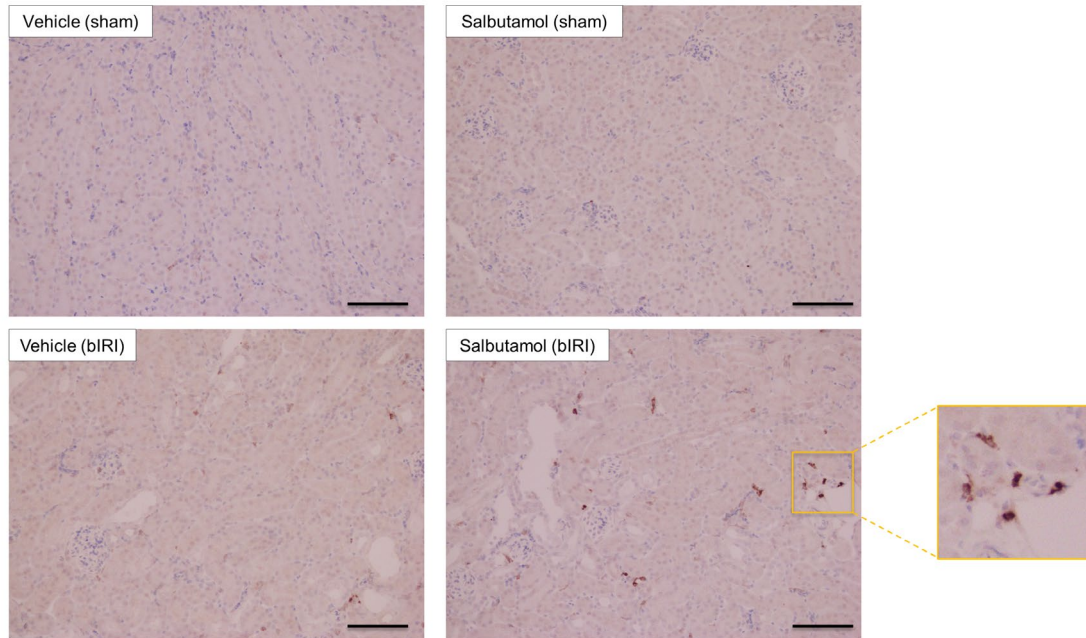


Supplemental Figure 9. Cell-type marker gene expression levels for unbiased clustering of single-cell RNA sequencing data

(A) The expression level of kidney androgen-regulated protein (*Kap*), a representative marker of proximal tubules in the S3 segment (PT [S3]), is visualized on t-distributed stochastic neighbor embedding (tSNE) plots of the single-cell RNA sequencing data in Figure 7.

(B) The expression levels of two representative macrophage markers (*Cd68* and lysozyme M [*LysM*]) are visualized on tSNE plots of the single-cell RNA sequencing data in Figure 7.

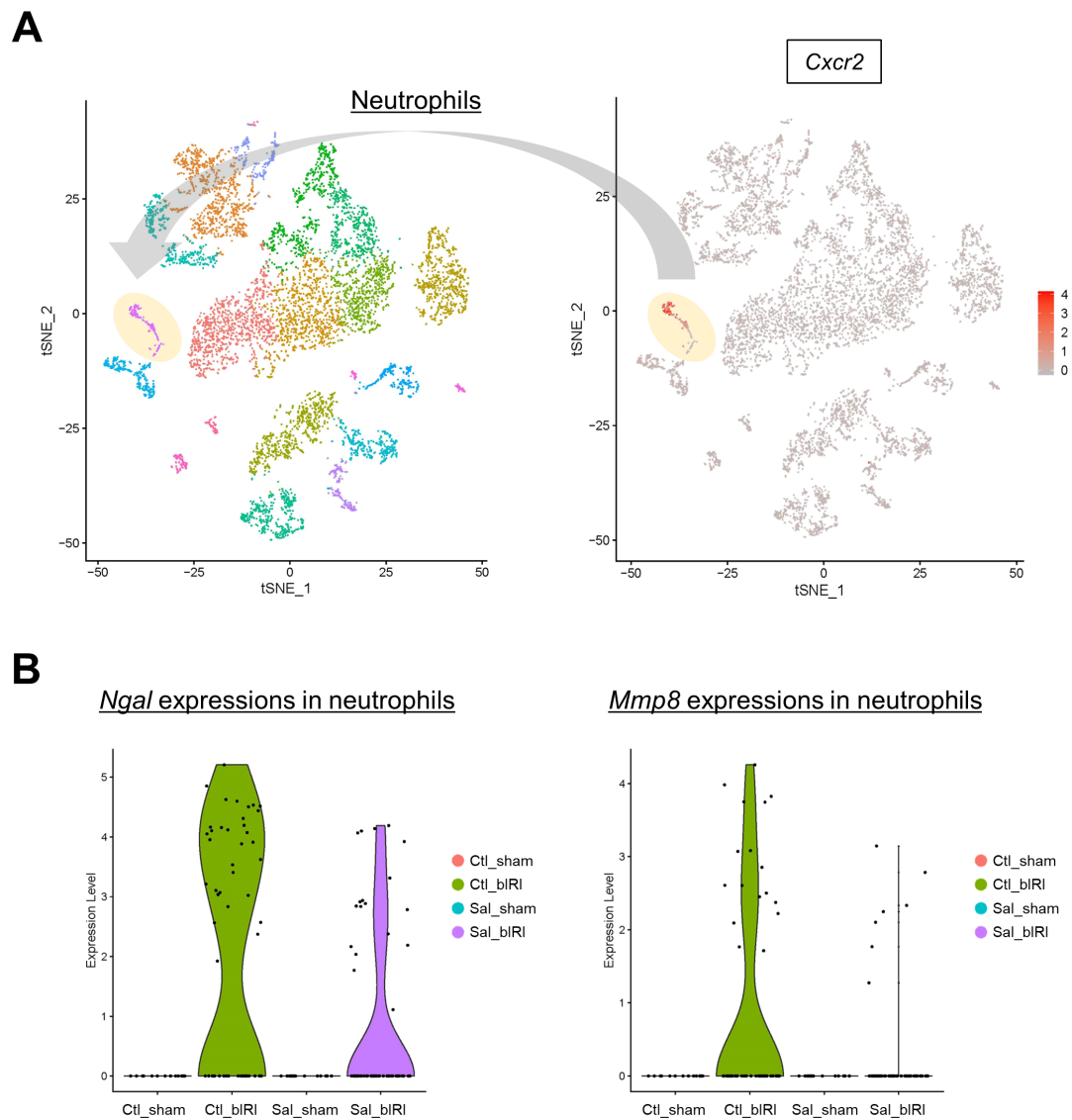
Supplemental Figure 10



Supplemental Figure 10. Immunostaining of T-cell immunoglobulin and mucin domain 3 on renal tissues of the adoptive transfer experiment

T-cell immunoglobulin and mucin domain 3 (Tim3) immunostaining of the renal tissues in the adoptive transfer experiment (Figure 6) is shown (Scale bar = 100 μ m). Tim3-positive cells were particularly accumulated in the renal tissue after renal bilateral ischemia/reperfusion injury (bIRI) followed by the adoptive transfer of salbutamol-treated macrophages.

Supplemental Figure 11



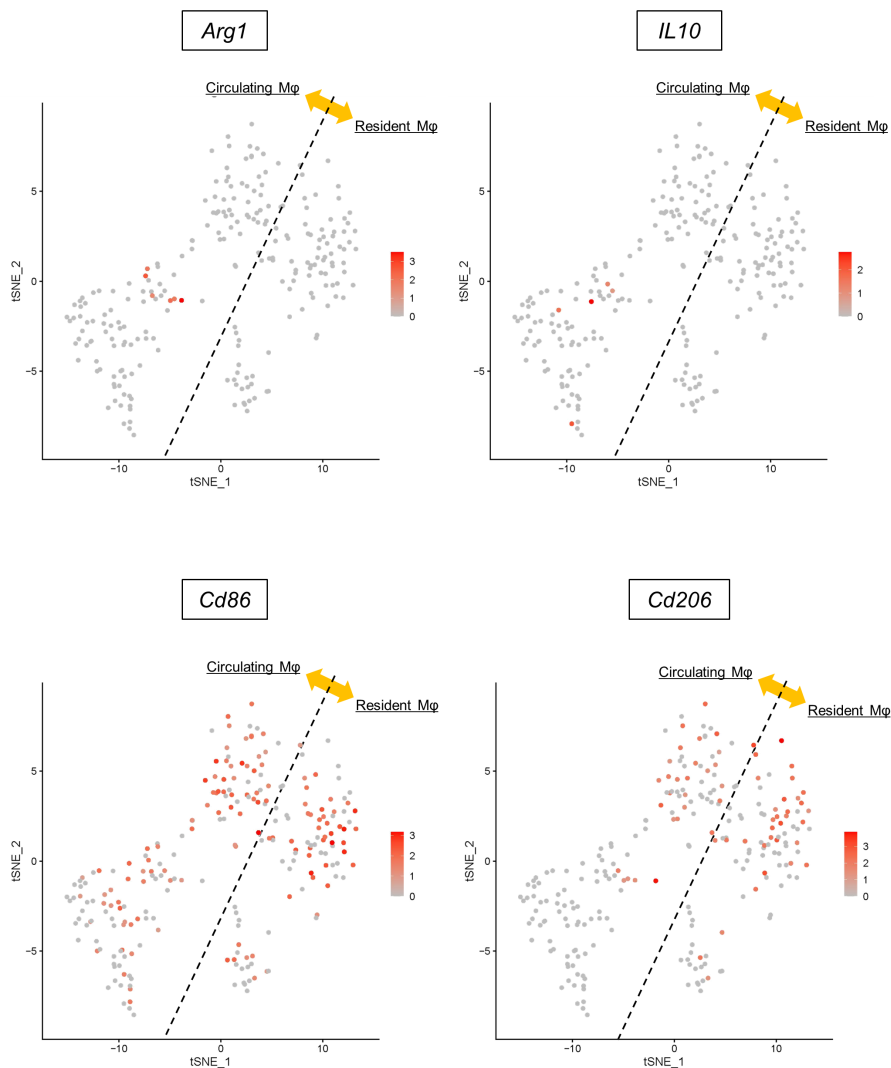
Supplemental Figure 11. Assessment of infiltrating neutrophils in the single-cell RNA sequencing data

The expression of C-X-C chemokine receptor type 2 (*Cxcr2*) identified the neutrophil cluster in the single-cell RNA sequencing data. The total number of cells in this cluster is as follows: 13 cells (Ctl_sham), 55 cells (Ctl_bIRI), 13 cells (Sal_sham), and 62 cells (Sal_bIRI). The expressions of pro-inflammatory markers such as neutrophil gelatinase-

associated lipocalin (*Ngal*) and matrix metalloproteinase 8 (*Mmp8*) in this cluster showed that the phenotype of infiltrating neutrophils might be different between Ctl_bIRI and Sal_bIRI conditions.

Ctl_sham: sham operation followed by vehicle-treated macrophage transfer, Ctl_bIRI: bilateral ischemia/reperfusion injury (bIRI) followed by vehicle-treated macrophage transfer, Sal_sham: sham operation followed by salbutamol-treated macrophage transfer, Sal_bIRI: bIRI followed by salbutamol-treated macrophage transfer.

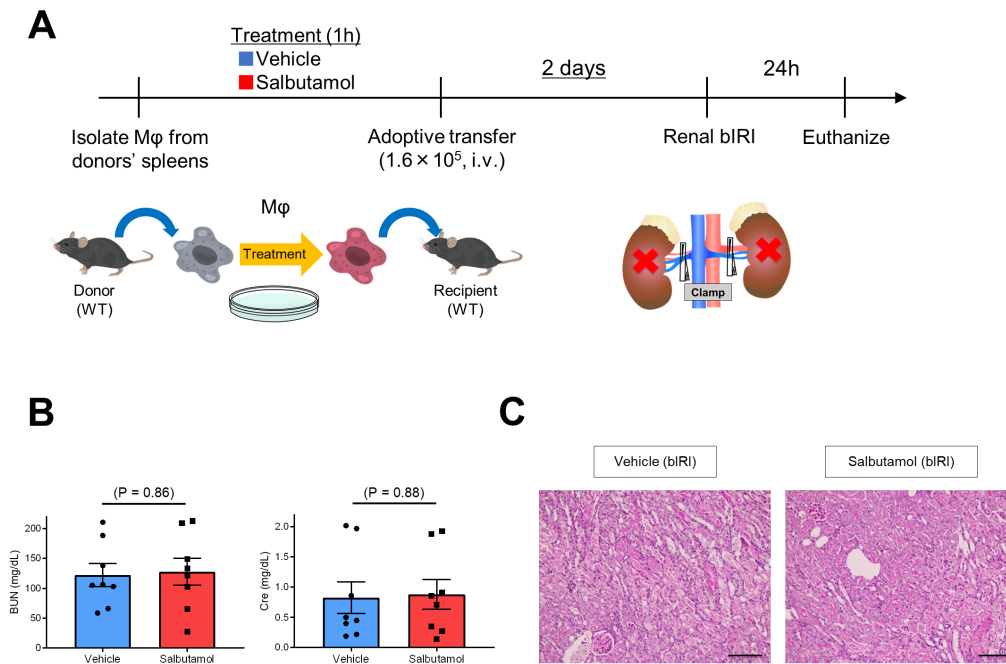
Supplemental Figure 12



Supplemental Figure 12. M1/M2 marker gene expression levels on the macrophage sub-clustering data in the single-cell RNA sequencing

The expressions of representative M1/M2 markers on the macrophage (Mφ) cluster are shown on the t-distributed stochastic neighbor embedding (tSNE) plots. Arginase 1 (*Arg1*) or interleukin-10 (*IL10*)-positive macrophages were small in number and preferentially distributed on the left side (circulating macrophages). In contrast, *Cd86* (M1 marker) or *Cd206* (M2 marker)-positive macrophages were large in number and distributed on both sides (circulating and tissue-resident macrophages).

Supplemental Figure 13



Supplemental Figure 13. The adoptive transfer of salbutamol-treated macrophages two days before renal ischemia/reperfusion injury does not provide protection

(A) The study protocol is shown. Salbutamol-treated macrophages (M ϕ) from donor mice treated with salbutamol were adoptively transferred to recipient mice 2 days before bilateral ischemia/reperfusion injury (bIRI). Blood and kidney samples were obtained 24 h after bIRI.

(B) The blood urea nitrogen (BUN) and plasma creatinine (Cre) levels as well as (C) histological tubular injury did not differ between the vehicle and salbutamol groups ($n = 8$), suggesting that the protective effects of adoptive transfer is not maintained for two days.

All data are presented as means \pm standard error of the mean. Statistical comparisons were analyzed by an unpaired two-tailed t test.

Supplemental Table 1. Primer sequences for the quantitative real-time polymerase chain reactions

Supplemental Table 2. A list of the marker genes of each cluster in the single-cell RNA sequencing

The marker genes sorted by average log fold-change (FC) of each cluster in the single-cell RNA sequencing are presented.

Supplemental Table 3. A list of the 37 genes commonly selected in the RNA sequencing from the three *in vitro* models

The expression of each gene is presented as log (fragments per kilobase of transcript per million mapped fragments [FPKM] + 0.001).

(Supplemental Tables were prepared as Excel files.)